

THE CURVE SHORTENING FLOW FOR CURVES OF FINITE TOTAL (ABSOLUTE) CURVATURE

PATRICK GUIDOTTI

ABSTRACT. We revisit the well-known Curve Shortening Flow for immersed curves in the d -dimensional Euclidean space. We exploit a fundamental structure of the problem to derive a new global construction of a solution, that is, a construction that is valid for all times and is insensitive to singularities. The construction is characterized by discretization in time and the approximant, while still exhibiting the possible formation of finitely many singularities at a finite set of singular times, exists globally and is well behaved and simpler to analyze than a solution of the CSF. A solution of the latter is obtained in the limit. Estimates for a natural (geometric) norm involving length and total absolute curvature allow passage to the limit. Many classical qualitative results about the flow can be recovered by exploiting the simplicity of the approximant and new ones can be proved. The construction also suggests a numerical procedure for the computation of the flow which proves very effective as demonstrated by a series of numerical experiments scattered throughout the paper.

1. INTRODUCTION

The so-called Curve Shortening Flow is a special case of a geometric evolution equation known as the Mean Curvature Flow whereby a spatial curve is moved in normal direction with a speed given by its curvature. There is a vast literature concerning the MCF even in its simplest CSF form. In this paper we mainly consider the CSF for immersed initial curves even though some of the results are interesting even in the embedded case. The contributions of this paper are a new construction of the solution for the flow in \mathbb{R}^d ($d \geq 2$) by a semi-discrete approximation procedure which generates approximating flows that can undergo singularity formation but are always globally defined in time. This is to be compared to the common perception since Grayson's work [12] that "The real difficulty lies in showing that the flow [CSF] is complete. One discovers quickly that this is equivalent to showing that the curvature remains bounded until the entire curve shrinks to a point." We argue that singularity formation is a natural phenomenon for the flow (even in its linearized form, as we shall see) and that, in a generalized sense, curvature does in fact not blow up until the extinction time of the flow (when the curve shrinks to a point) but merely occasionally concentrates. The issue of curvature blow up can be circumvented by resorting to various concepts of weak solution. This typically results in the loss of uniqueness (as is the case for Brakke's construction [7] applied to the CSF). The approximating flows constructed here are easier to analyze and allow us to prove qualitative and asymptotic properties of solutions and to gain insight into special solutions. Furthermore uniqueness holds in as far it holds for classical solutions of the CSF since the solutions obtained are classical away from singularities and continuous through the singularities. Last but not least the construction of the solutions suggests a natural discretization which turns out to yield an effective algorithm for the numerical computation of the flow.

Next we summarize important contributions to the understanding of the CSF. The embedded case was thoroughly analyzed in the ground-breaking contributions of Gage [10, 9] and, later, of Gage and Hamilton [8], in the convex case, and of Grayson [11], in the general case. In the case of immersed curves, seminal contributions are due to Angenent [4, 6]. In these papers the author obtains a variety of results concerning solutions of a class of geometric (curve) evolutions on two dimensional surfaces of

Key words and phrases. Curve shortening flow, mean curvature flow, existence of solutions, numerical computation, special solutions.

which the curve shortening flow is an example. Abresch and Langer [1] characterize all closed curves that evolve homotetically and show that they serve as the model for the asymptotics in the singularity for curves which shrink to a point in way such that the (normalized) curvature converges in L^1 . Along these lines Huisken [14] and Angenent [5] show that planar curves which develop type-I singularities are asymptotic to an Abresch-Langer curve. A result of Altschuler [2] shows that space curves exhibit planar asymptotic behavior (hence of Abresch-Langer type) in the case of type-I singularities. For Type-II singularities, a blow-up of the solution is shown to be asymptotic to the Groom Reaper. Halldorsson [13] characterizes all self-similar solutions of the planar CSF. For completeness we also mention the work of Altschuler and Grayson [3] that approximates the planar CSF by a regularized flow for curves in \mathbb{R}^3 that exhibits no singularities and exist globally in time.

2. THE EQUATION

In order to formulate the problem mathematically in a way that is convenient for the purposes of this paper, we fix some notation. The set $\mathcal{C} = \mathcal{C}(\mathbb{R}^d)$ of all closed curves in \mathbb{R}^d ($d \in \mathbb{N}$) is defined by

$$\mathcal{C}(\mathbb{R}^d) = \left\{ X : [0, 1] \rightarrow \mathbb{R}^d \mid X \in W_\pi^{1,\infty}([0, 1], \mathbb{R}^d), X_r \in BV_\pi([0, 1], \mathbb{R}^d) \right\}, \quad (2.1)$$

where the subscript π indicates that the parametrizations are periodic. By BV we denote the space functions of bounded variation. We shall also use the notation SBV for the space of BV functions for which the singular part of their derivative consists only of vector-valued Dirac masses. We can assume without loss of generality that all parametrizations have common domain of definition $[0, 1] =: I \cong \mathbb{S}^1$. Notice that elements of $\mathcal{C}(\mathbb{R}^d)$ are not necessarily immersed. We therefore denote by $\mathcal{IC}(\mathbb{R}^d)$ the subset of immersed curves. By immersion we mean that X , while allowed to exhibit singularities (discontinuities of the tangent vector), is still an everywhere local injection. For any $X \in \mathcal{C}$, $X(I)$ is a rectifiable curve and its arc-length is given by

$$s = \overline{\varphi}_X(r) = \int_0^r |X'(\rho)| d\rho, \quad r \in I.$$

Its length $\overline{\varphi}_X(1)$ is denoted by $L(X)$. Any curve in $\mathcal{C}(\mathbb{R}^d)$ can be parametrized *normally*, i.e. it possesses a parametrization $Y \in \mathcal{C}(\mathbb{R}^d)$ for which $|Y'| \equiv L(X)$. Given a parametrization X , we denote its normal reparametrization $X \circ \varphi_X^{-1}$ by $R(X)$. Notice that

$$R : \mathcal{C}(\mathbb{R}^d) \rightarrow \mathcal{C}(\mathbb{R}^d), \quad X \rightarrow X \circ \varphi_X^{-1},$$

is a nonlinear operator and that we define

$$\varphi_X = \frac{1}{L(X)} \overline{\varphi}_X : I \rightarrow I.$$

We identify parametrizations that only differ by a continuous, piecewise smooth change of variables $\varphi : [0, 1] \rightarrow [0, 1]$ and allow for orientation reversing change of variables as they do not alter the evolution of the curve under the Curve Shortening Flow. While this removes some ambiguity, there are still distinct immersed, non-embedded, curves that share the same trace set (see e.g. Figure 3). In this sense, an immersed curve is an equivalence class of parametrizations and, given X , we sometimes denote the corresponding curve by $[X]$ but, more often, abuse notation and simply speak of the curve X conflating the parametrization at hand with the equivalence class it represents. We observe, as pointed out e.g. in [4], that a curve's normal parametrization is unique up to a rigid transformation of \mathbb{S}^1 , so that, given a normal parametrization X , the only other equivalent normal parametrizations Y are given by

$$Y(s) = X(s + \theta) \text{ or by } Y(s) = X(-s + \theta), \quad s \in I,$$

for some $\theta \in I$ and where addition is interpreted modulo 1. The tangent line (not vector) to a curve $[X]$ at one of its points is either well-defined or experiences a discontinuity. The tangent vector depends

on the direction of parametrization. If $X' \in \text{SBV}_\pi(I)$, it is well-defined or undergoes a jump for any chosen representative X of a curve $[X]$. In particular

$$\lim_{r \rightarrow r_0 \pm} X'(r)$$

exist for every $r_0 \in I$. We say that a curve is *essentially* parametrized by X if there is no interval $J \subset I$ on which X is constant. We denote the space of (equivalence classes of) [immersed] curves described above by $\mathcal{C}_e(\mathbb{R}^d)$ $[\mathcal{IC}_e(\mathbb{R}^d)]$ and notice that each equivalence class has a normally and essentially parametrized representative. On $\mathcal{C}_e(\mathbb{R}^d)$, we can use the norm given by

$$\|X\|_C = \|X\|_\infty + \|X_r\|_{L^1} + \|X_{rr}\|_{\mathcal{M}}, \quad X \in \mathcal{C}_e(\mathbb{R}^d), \quad (2.2)$$

where the last term denotes the $|X_{rr}|(I)$ for the total variation measure $|X_{rr}|$ of the vector valued measure X_{rr} . One has of course to use the corresponding quotient norm for the equivalence classes of parametrizations but we shall see later that a more geometric choice of norm can be made that is independent of parametrization and thus behaves like a quotient norm.

Example 2.1. *A simple example of a non-immersed curve of the kind considered that we will revisit later is a doubly covered segment. Given two points $X^i \in \mathbb{R}^d$ ($i = 1, 2$), a normal and essential parametrization of the doubly covered segment connecting them is given by*

$$X(s) = \begin{cases} (1-2s)P_0 + 2sP_1, & s \in [0, \frac{1}{2}), \\ (2-2s)P_1 + (2s-1)P_0, & s \in [\frac{1}{2}, 1). \end{cases} \quad (2.3)$$

Notice that $|X_s(s)| = 2|P_1 - P_0| = L(X)$ and that

$$X_s = 2(P_1 - P_0)\chi_{[0, \frac{1}{2})} + 2(P_0 - P_1)\chi_{(\frac{1}{2}, 1)}, \quad X_{ss} = 4(P_1 - P_0)[\delta_0 - \delta_{\frac{1}{2}}].$$

For a parametrized curve X , its curvature (vector) is defined by

$$k = \frac{1}{L^2(X)} \partial_{ss} R(X).$$

This curvature coincides with the usual curvature vector of a curve in the smooth case and R becomes the identity for normally parametrized curves. We have that

$$k = k^r + k^s,$$

where $k^r \in L^1_\pi(I)$ is the regular part and $k^s \in \mathcal{M}_\pi(I)$ is the singular part consisting of vector-valued Dirac measures, if $X_s \in \text{SBV}_\pi$. The case of countably many singularities is not excluded but, in this paper, only the finite case will play a role. Then $R(X)_s = \frac{L(X)}{|X_r|} X_r$ only has a finite number of jump discontinuities.

Example 2.2. *For the doubly covered segment we have that*

$$k(X) = \frac{P_1 - P_0}{|P_1 - P_0|^2} [\delta_0 - \delta_{\frac{1}{2}}].$$

The smooth *mean curvature flow* for a time dependent family of curves $X = X(t, \cdot)$, $t \geq 0$, is given by

$$V(X) = \kappa(X),$$

where $V(X)$ is the so-called normal velocity of X and $\kappa(X) = \nu(X) \cdot k(X)$ (see [4]). In this formulation the sign of κ depends on the choice of the normal (in relation to the orientation of the curve) and on the orientation chosen for the ambient space. Working with the curvature vector, as we will, avoids this issue. A solution of the CSF is obtained if solutions of $X_t = k(X)$ can be produced. Notice that

$$R : \mathcal{C}_e(\mathbb{R}^d) \rightarrow \mathcal{C}_e(\mathbb{R}^d), \quad X \rightarrow X \circ \varphi_X^{-1},$$

is well-defined since φ_X is strictly increasing for $X \in \mathcal{C}_e(\mathbb{R}^d)$ even if $|X_r|$ can have some zeros. From now on, we shall refer to the PDE system

$$\begin{cases} \partial_t X = \frac{1}{L^2(X)} \partial_{ss} R(X), & t > 0, \\ X(0) = X^0 \in \mathcal{C}_e, \end{cases} \quad (2.4)$$

as the *curve shortening flow (CSF)* for the initial curve X^0 . It is apparent that the nonlinear nature of (2.4) only stems from the normal reparametrization operator R and the length operator L . It can be verified that

$$R(\partial_t X) \neq \partial_t R(X),$$

in general and, therefore, no simple equation can be derived if X is replaced by $R(X)$. It is, however, an important observation that

$$R(X_t) \cdot \nu(X) = R(X)_t \cdot \nu(X).$$

Here and above X_t is a tangent vector(field) at X to the manifold of immersed curves and $R(X_t) = X_t \circ \varphi_X^{-1}$ is the natural extension of R to the tangent space at X . It follows that $[R(X)] = [X]$ can be “updated” using the alternative equation

$$R(X)_t = \frac{1}{L^2(R(X))} \partial_{ss} R(X),$$

while still yielding a solution of the mean curvature flow, which only involves the normal velocity $V(X)$ as observed above. This fact is the essential motivation for the construction of the solution and for the discretization presented later as well as the reason for the efficacy and simplicity of the numerical scheme. We reiterate, however, that it is not possible to simply replace the CSF (2.4) by the equation

$$Y_t = \frac{1}{L^2(Y)} \partial_{ss} Y$$

for $Y = R(X)$, because this equation does not preserve the normalized length of a parametrization.

Notice that L is a nonlinear function of X but $L(X) = L(R(X)) = |\partial_s R(X)|$ only depends on time.

Remark 2.3. *We point out that Definition (2.4) of the CSF is more general than the usual differential geometric definition. It is solely based on the existence of a generalized curvature vector. The latter is sometimes defined even when the actual curvature is not. If a curve is smooth, then we have the relation $\kappa(X) = k(X) \cdot \nu(X)$. In the non-smooth case, take for instance a square of unit length and normal-length parametrized by*

$$X(s) = \begin{cases} (s, 0), & s \in [0, \frac{1}{4}), \\ (\frac{1}{4}, s - \frac{1}{4}), & s \in [\frac{1}{4}, \frac{1}{2}), \\ (\frac{3}{4} - s, \frac{1}{4}), & s \in [\frac{1}{2}, \frac{3}{4}), \\ (0, 1 - s), & s \in [\frac{3}{4}, 1). \end{cases}$$

Then $X_{ss} = (1, 1)\delta_0 + (-1, 1)\delta_{\frac{1}{4}} + (-1, -1)\delta_{\frac{1}{2}} + (1, -1)\delta_{\frac{3}{4}}$ is a measure and the unit normal is merely L^∞ and these can therefore not be multiplied together. Likewise the Euclidean norm of X_{ss} cannot be computed.

Motivated by the above example, we investigate curvature and total curvature in the context of curves with singularities, starting in the plane. For smooth curves, it is known that the total curvature κ_{tot} of a curve parametrized by X can be computed by

$$\kappa_{tot}(X) = \int_0^{L(X)} |\partial_{ss} X| d\bar{\sigma} = \frac{1}{L(X)} \int_0^1 |\partial_{ss} X| d\sigma,$$

where \bar{s} is the arc-length and s the normalized length, i.e. $\bar{s} = L(X)s$. In the smooth case this is equivalent to

$$\kappa_{tot}(X) = \int_0^L |\partial_{\bar{s}}\theta| d\bar{\sigma} = \int_0^1 |\partial_s\theta| d\sigma,$$

where $\theta(\bar{s}) = \arccos(\partial_{\bar{s}}X \cdot e_1) = \arccos(\frac{1}{L}\partial_sX \cdot e_1)$ measures the angle the tangent vector makes with the vector e_1 along the curve. This is an immediate consequence of writing

$$\partial_{\bar{s}}X = (\cos(\theta(\bar{s})), \sin(\theta(\bar{s}))), \quad \partial_sX = L(\cos(\theta(s)), \sin(\theta(s))),$$

and computing $|\partial_{\bar{s}\bar{s}}X| = |\partial_{\bar{s}}\theta(\bar{s})|$. In particular it always holds that

$$\int_0^L |\partial_{\bar{s}\bar{s}}X| d\bar{\sigma} = \int_0^L |\partial_{\bar{s}}\theta| d\bar{\sigma}. \quad (2.5)$$

In the singular case, it would seem natural to replace the length of the curvature vector $|\partial_{\bar{s}\bar{s}}X|$, now a Radon measure, with its variation (measure) $|\partial_{\bar{s}\bar{s}}X|$ and total curvature by

$$|\partial_{\bar{s}\bar{s}}X|([0, L)) = \frac{1}{L}|\partial_{ss}X|(I).$$

It, however, turns out that identity (2.5) is no longer valid for singular curves. Take for instance the square discussed in Remark 2.3 to see that

$$\partial_{\bar{s}}X = e_1\chi_{[0, \frac{1}{4})} + e_2\chi_{[\frac{1}{4}, \frac{1}{2})} - e_1\chi_{[\frac{1}{2}, \frac{3}{4})} - e_2\chi_{[\frac{3}{4}, 1)}.$$

Then

$$\partial_{\bar{s}\bar{s}}X = (e_1 + e_2)\delta_0 + (e_2 - e_1)\delta_{\frac{1}{4}} + (-e_1 - e_2)\delta_{\frac{1}{2}} + (e_1 - e_2)\delta_{\frac{3}{4}},$$

which has a compelling geometric interpretation, and

$$|\partial_{\bar{s}\bar{s}}X| = \sqrt{2} \sum_{i=0}^3 \delta_{\frac{i}{4}}, \quad |\partial_{\bar{s}\bar{s}}X|(I) = 4\sqrt{2}.$$

On the other hand,

$$\theta = 0\chi_{[0, \frac{1}{4})} + \frac{\pi}{2}\chi_{[\frac{1}{4}, \frac{1}{2})} + \pi\chi_{[\frac{1}{2}, \frac{3}{4})} + \frac{3\pi}{2}\chi_{[\frac{3}{4}, 1)}, \quad \partial_{\bar{s}}\theta = \frac{\pi}{2} \sum_{i=0}^3 \delta_{\frac{i}{4}},$$

so that

$$|\partial_{\bar{s}}\theta|(I) = 2\pi,$$

which is indeed the total curvature of the square. We conclude that $\partial_{\bar{s}\bar{s}}X$ and $\partial_{\bar{s}}\theta$, while essentially containing the same information and being useful quantities, are not related in the obvious way they are for smooth curves. This is due to the fact that nonlinear operations are involved in the transition between these quantities that are not well-defined for measures. For the singular curves considered in this paper, we shall from now on define the curvature vector by $\frac{1}{L^2}\partial_{ss}X$ or $\partial_{\bar{s}\bar{s}}X$ and total curvature by

$$\kappa_{tot}(X) = \frac{1}{L(X)}|\partial_{ss}X|(I). \quad (2.6)$$

At least in $d = 2$, one could use the alternative definition

$$\kappa_{tot}(X) = \int_I |(d\theta)^r| + |(d\theta)^s|(I)$$

where $(d\theta)^r$ and $(d\theta)^s$ are the regular and singular (jump) part of $d\theta$, respectively. The difference between $|\partial_{ss}X|(I)$ and $|\partial_s\theta|(I)$ for singular curves in \mathbb{R}^d has been discussed before by [17]. The unit tangent to a curve traces a curve in \mathbb{S}^{d-1} , the so-called tantrix. Its length as a (discontinuous) curve in \mathbb{S}^{d-1} corresponds to $|\partial_s\theta|(I)$, whereas its length as a curve in \mathbb{R}^d yields $|\partial_{ss}X|(I)$. The former has the advantage of coinciding with the limit of the total curvature of approximating polygons (defined as their total turning angle). Notice that, for smooth curves, both quantities coincide since,

infinitesimally, the ambient space distance and the unit sphere distance coincide and the two diverge only when singularities are present. Clearly these total curvatures are either both finite or both infinite and there is a simple relation between them as explained in [17, Section 3]. In the same paper, it is also shown, following [16], that the total curvature of a curve Γ in \mathbb{R}^d can be defined by

$$\kappa_{tot}(\Gamma) = \sup_{\mathbb{P} < \Gamma} \kappa_{tot}(\mathbb{P}),$$

where the supremum is taken over all possible polygons generated by selecting an (ordered) sequence $\mathbb{P} = (X_0, \dots, X_{m-1})$ of points from the curve Γ , and

$$\kappa_{tot}(\mathbb{P}) = \sum_{i=0}^{m-1} \theta_i,$$

where θ_i is the turning angle at X_i , i.e. the angle between the unit vector in the direction determined by X_{i-1} and X_i , and that in the direction determined by X_i and $X_{(i+1) \bmod m}$. We shall make use of this fact to compute a numerical approximation of this quantity later in the paper.

With total absolute curvature in hand, we can introduce the following more geometric norm on the space $\mathcal{C}(\mathbb{R}^d)$ defined by

$$\|X\|_{\mathcal{G}} = \|X\|_{\infty} + L(X) + \kappa_{tot}(X) \quad (2.7)$$

for the curve with parametrization $X \in \mathcal{C}_e(\mathbb{R}^d)$. Notice that its value is independent of the chosen parametrization within the same equivalence class. In particular $\|X\|_{\mathcal{G}} = \|R(X)\|_{\mathcal{G}} = \|R(X)\|_{\mathcal{C}}$ and so this quantity bounds the quotient norm of X .

3. STEADY STATES

Among the shapes that evolve only by rescaling there may be some that remain normally parametrized if they are initially normally parametrized, i.e. curves for which it holds that $R((X(t))) = X(t)$ whenever $R(X^0) = X^0$. Such curves satisfy the quasi-linear equation

$$\partial_t X = \frac{1}{L^2(X)} \partial_{ss} X.$$

In this case, we have that $X(t) = r(t)X^0$, where $r(0) = 1$, so that the equation becomes

$$\dot{r}(t)X^0 = \frac{1}{L_0^2 r(t)} \partial_{ss} X^0,$$

where $L_0 = L(X^0)$. By separation of variables, it must hold that

$$\begin{cases} \partial_{ss} X^0 = \mu X^0, \\ L_0^2 \dot{r}(t)r(t) = \mu, \quad r(0) = 1, \end{cases} \quad (3.1)$$

for some $\mu \in \mathbb{R}$. Then $\mu = -4\pi^2 n^2$ for $n \in \mathbb{N} \cup \{0\}$ and

$$X^0 = a \cos(2\pi ns) + b \sin(2\pi ns), \quad r(t) = \sqrt{1 + 2 \frac{\mu}{L_0^2} t},$$

for some $a, b \in \mathbb{R}^d$. If $n = 0$, then the only (connected) solution would correspond to a constant point (where $r(0) = 0$) but this solution is not considered as it will always be assumed that $L_0 > 0$, when it needs to hold that $r(0) = 1$. For $n \in \mathbb{N}$, it must hold that

$$|-2\pi na \sin(2\pi ns) + 2\pi nb \cos(2\pi ns)|^2 = L_0^2, \quad s \in I,$$

which implies that

$$4\pi^2 n^2 [|a|^2 \sin^2(2\pi ns) + |b|^2 \cos^2(2\pi ns)] - 8\pi^2 n^2 a \cdot b \sin(2\pi ns) \cos(2\pi ns) \equiv L_0^2.$$

This entails that

$$|a| = |b| = \frac{L_0}{2\pi n} \text{ and that } a \cdot b = 0.$$

The curve is therefore a circle traversed n -times that lies in the plane spanned by a and b . If that circle is normalized to have length 1, then the curve has length $2\pi n$ and a, b are orthonormal. Moreover, this n -fold circle shrinks to a point when

$$\sqrt{1 - 2\frac{4\pi^2 n^2}{4\pi^2 n^2}t} = \sqrt{1 - 2t} = 0,$$

i.e. when $t = \frac{1}{2}$. It is known that simple closed curves evolve reducing the enclosed area at the constant rate 2π . Thus the multiply traversed circle decreases its length at a speed that is higher so as to make the extinction time the same for all $n \in \mathbb{N}$, in this simple case of a non-simple curve.

Remark 3.1. *There are self-similar solutions, even when considering closed curves only, which evolve by rescaling but for which $R(X(t)) \neq X(t)$ even if $R(X^0) = X^0$. All planar curves evolving in this way have been identified in [13] by the use an ODE system. They include the curves already known from [1] which are closed curves of finite length that shrink homotetically. These are characterized by the fact that the parametrization does not remain normal along (2.4) and hence*

$$X(t, s) = r(t)X^0(\varphi(t, s)), \quad s \in I, \quad t \geq 0,$$

where $\varphi(0, s) = s$ for $s \in I$. The CSF in this cases reduces to

$$\dot{r}X^0 \circ \varphi \cdot \nu^0 \circ \varphi = \frac{1}{r}k^0 \circ \varphi \cdot \nu^0 \circ \varphi,$$

or, equivalently, to

$$\dot{r}rX^0 \cdot \nu^0 = k^0 \cdot \nu^0.$$

By rescaling X^0 if necessary, we can assume that $\dot{r}r = -1$ and thus homotetically evolving curves must satisfy

$$X^0 \cdot \nu^0 + k^0 \cdot \nu^0 = 0.$$

From here an ODE can be derived for the curvature κ^0 which allows for the classification of all possible solutions. A thorough discussion is found e.g. in [15, Appendix E].

Remark 3.2. *Assuming smoothness, the CSF flow is equivalent to the system*

$$\begin{cases} X_t = \Sigma_* k(X), & k(X) = \frac{1}{L^2} R(X)_{ss}, \\ \sigma_t = \sigma \left[\int_0^1 k(X) \cdot k(X) - \Sigma_* k(X) \cdot \Sigma_* k(X) \right], & s = \int_0^r \sigma(t, \rho) d\rho =: \Sigma(r), \\ L_t = -L \int_0^1 k(X) \cdot k(X), \end{cases}$$

where $X(0) = X^0$, $L(0) = L(X^0)$, and $\sigma(0, r) = |X_r^0(r)|$, $r \in I$. This system is obtained using the well-known equations that can be derived for the CSF as they can be found in [8, Section 3], for instance. It shows that a solution is continuously undergoing reparametrization unless its curvature is constant.

4. CONSTRUCTION OF A SOLUTION

In order to obtain a solution to the CSF for any given initial datum in $\mathcal{C}_e(\mathbb{R}^d)$ and in order to derive an effective numerical approach to its solution (see later) we will heavily rely on formulation (2.4).

The idea is to linearize (2.4) by intertwining reparametrizations and small time interval evolutions by the linear heat equation while keeping track of singularity formation. We define recursively

$$\begin{cases} X^n(t) = e^{\frac{t-kh}{L^2(X^n(kh))} \partial_{ss}} R(X^n(kh)), & t \in [kh, (k+1)h), \quad k \geq 0, \\ X^n(0) = X_0 = R(X_0), \end{cases} \quad (4.1)$$

where $X^n(kh)$ has been determined in the previous step. We point out a last time that this evolution is an evolution for the immersed curve $[X^0]$ and that the use of the operator R preserves the equivalence

class, i.e. the curve. Here we switched the notation for the initial parametrized curve to X_0 , we set $h = \frac{1}{n}$ for $n \in \mathbb{N}$ and

$$L(X^n(kh)) = \int_0^1 |\partial_r X^n(kh)| d\rho = |\partial_s R(X^n(kh))|,$$

During this evolution it is possible to encounter (singular) times t_{sing} at which $|\partial_s X^n(t_{sing})| = 0$ at one or several parameter values. At such times the evolving curve experiences one or more singularities. In any time interval of length h (and overall) this happens at most a finite number of times as explained below. For future use, we also define

$$Y^n(t) = \begin{cases} X^n(t), & t \notin h\mathbb{N} \\ e^{\frac{h}{L^2(X^n(kh))} \partial_{ss}} R(X^n(t-h)), & t \in h\mathbb{N}. \end{cases}$$

Letting $\Gamma^n(t)$ denote image set of $X^n(t)$, $Y^n(t)$ is a smooth (analytic) parametrization of it for each time $t > 0$.

We interpret X^n (or Γ^n) as the n -th interpolant (approximant) to the CSF and collect some important properties it enjoys in the next sections. In particular, (4.1) defines an orbit of curves that depends continuously on time as does its length. The tangent vector(field) to the orbit is piecewise smooth and bounded (in the appropriate sense). The approximant does converge (as $n \rightarrow \infty$) to a globally defined limit X , which becomes constant (the curve shrinks to a point) in finite time and satisfies the CSF equation up to a finite number of singular times (that include the extinction time).

Remark 4.1. *The function $Y^n(t)$ satisfies a linear heat equation for all $t \neq kh$, $k \in \mathbb{N}$ and $Y^n(kh)$ is the end value of a linear heat equation. It follows that $V + MY^n(t)$ also satisfies a linear heat equation for any $V \in \mathbb{R}^d$ and $M \in \mathbb{R}^{d \times d}$. In particular any rigid change of coordinates in the ambient space yields parametrizations that satisfy the same linear heat equation.*

4.1. Extremity Points and Singularities.

Definition 4.2. *A point P on a curve smoothly parametrized by X is called an extremity point if $\partial_s X^i(r_0) = 0$ for at least one $i \in \{1, \dots, d\}$ and $X(r_0) = P$. Singular points are special extremity points where all components of $\partial_s X$ vanish simultaneously. The set of extremity points is denoted by $\mathcal{E}(X)$. We say that a curve Γ has finitely many extremity points if there is a coordinate system (an origin and an orthonormal basis) in which it admits a parametrization X with $\mathcal{E}(X) < \infty$.*

Remarks 4.3. (a) *We include inflection points of components in the definition of extremity point for simplicity, but, minima and maxima are the interesting critical points for the evolution. This is related to the fact that diffusion instantaneously removes inflection points.*

(b) *A singularity point along a smoothly and essentially parametrized curve is a special extremity point where all components of the tangent vector vanish simultaneously.*

(c) *If a curve is parametrized in a non-smooth way, then extremity points also include local maxima and minima at which the parametrization is not differentiable.*

(d) *The only way to parametrize about a singular point in a smooth manner is by “stalling” at the singularity. In this way all components of the parametrization must vanish at the singular points. Inflection points are generated in all components for which the singular point is not a local extremum.*

Proposition 4.4. *Given X_0 with finitely many extremity points, the number of extremity points of $X^n(t)$ is a non-increasing function of time, regardless of $n \in \mathbb{N}$.*

Proof. Under scalar diffusion maxima decrease and minima increase, while inflection points disappear instantaneously. As maxima and minima may merge during the evolution, the number of extremity points will not increase, as diffusion does not allow for the generation of new extrema. Inflection points can appear but only when extrema merge, like, e.g., when a minimum and a maximum coalesce. Non-smooth extremity points are instantaneously regularized, possibly turning into smooth extremal points. Notice that the operator R does not affect smooth extremity points, which are preserved after

reparametrization (their location in parameter space can of course change in the process). Extrema that do occur at singular points are also preserved by R , while inflection points that occur at a singular point may disappear when R is applied. \square

Remark 4.5. *If the initial curve is not smooth and possesses finitely many extremity points, we can assume without loss of generality that it be smooth and exhibit a finite number of extremity points by the regularizing effect of diffusion. As diffusion does not generate oscillations, a small time application of it removes singularities without affecting the (macroscopic) oscillatory properties of the initial components since we are assuming that they have at most finitely many extremity points.*

An important class of curves with finitely many extremity points (especially with respect to numerical approximation) is that of closed polygons $\mathbb{P} = (P_0, P_1, \dots, P_{n-1})$ for $n \in \mathbb{N}$ which we identify with the closed curve

$$(1 - (nt - i))P_i + (nt - i)P_{(i+1) \bmod n}, \text{ if } t \in \left[\frac{i}{n}, \frac{i+1}{n}\right), i = 1, \dots, n-1.$$

Proposition 4.6. *It holds that $|\mathcal{E}(\mathbb{P})| < \infty$ for any closed polygon \mathbb{P} .*

Proof. A polygon comprises a finite number of segments, each determining a direction $u_i = \overrightarrow{P_i P_{(i+1) \bmod n}}$ and an orthogonal hyperplane \mathcal{P}_i^\perp , $i = 1, \dots, n$. It suffices to choose a coordinate system, the basis vectors of which do not lie in any of these orthogonal planes. \square

4.2. Flow Singularities. During the flow X^n (arbitrary $n \in \mathbb{N}$), an initial curve is immediately regularized but can later develop singularities. They, however, must be very special in nature.

Proposition 4.7. *Regardless of $n \in \mathbb{N}$, the only possible singularities in the evolving curve X^n are cusps.*

Proof. At a singular time t_{sing}^n , the function $Z = Y_s(t_{sing}^n, \cdot)$ is analytic. Take a singular point of the corresponding curve. It can be assumed without loss of generality that the singular point occurs at the parameter value $s = 0$. Then, in a neighborhood, we have that

$$Z(s) = \sum_{n \geq 1} a_n s^n,$$

for coefficients $a_n \in \mathbb{R}^d$. Let $p \in \mathbb{N}$ be the smallest integer for which $a_p \neq 0$. A rigid transformation T can be found such that $Ta_p = |a_p|e_1$ and thus

$$TZ(s) = |a_p|e_1 s^p + \sum_{n \geq p+1} Ta_n s^n.$$

Then we have that

$$\lim_{s \rightarrow 0^\pm} \frac{TZ(s)}{|TZ(s)|} = \lim_{s \rightarrow 0^\pm} \frac{s^p}{|s|^p} e_1 = \begin{cases} \pm e_1, & p \text{ odd}, \\ e_1, & p \text{ even}. \end{cases}$$

As it is assumed that $s = 0$ corresponds to a singular point of the curve Z , p must be odd and the tangent points in direction $\pm T^{-1}e_1$ on either side of the singular point. This makes the singular point a cusp. In order to determine the exact type of cusp one can determine the smallest integer $q > p$ for which $(Ta_n)' \neq 0$, where $a' = (a^2, \dots, a^d)$ for $a \in \mathbb{R}^d$, and a rigid transformation \tilde{T} of \mathbb{R}^{d-1} such that $\tilde{T}(Ta_q)' = |a'_q|e_2' = |a'_q|e_1 \in \mathbb{R}^{d-1}$. Then the asymptotic properties of the cusp are determined by the parametrization

$$(|a_p|s^p + \sum_{n=p}^q (Ta_n)^1 s^n, |a'_q|s^q, 0, \dots, 0), s \simeq 0,$$

in the new coordinates determined by T and $\text{id}_{\mathbb{R}} \otimes \tilde{T}$. \square

Corollary 4.8. *Curves with kinks (changes of direction of less than π degrees) do not admit analytic parametrizations.*

Remark 4.9. *It cannot be excluded, in general, that a cusp singularity as described in the above proof be degenerate. This happens when only one component of the parametrization is non-zero (in the proper coordinates). This means that the cusp does not open. This is the case, for instance, for the two cusps of a doubly covered segment. Such a degenerate loop can, however, not appear on an immersed curve.*

Remark 4.10. *It is an interesting observation worth further investigation that, for the kind of curves considered here, the tangent line (as opposed to the tangent vector) is well-defined at each point. Indeed a jump of π degrees in the direction of the tangent vector does not represent a discontinuity in the tangent line (only a discontinuity of its orientation).*

Proposition 4.11. *If X_0 has at most finitely many extremity points, i.e. if $\mathcal{E}(X_0) < \infty$, then the flow X^n experiences singularities in at most finitely many singular times, i.e. times t_{sing} at which $\Gamma^n(t_{\text{sing}})$ has at most finitely many cuspidal points.*

Proof. We can assume that X_0 be smooth and normally parametrized. The initial curve has at most finitely many extremity points, i.e. zeros in any of the components of $\partial_s X_0$. Singularities are formed when $|\partial_s Y^n(t, \cdot)|$ vanishes at some parameter value s_0 and (singular) time t_{sing} . We already observed that inflection points immediately disappear and cannot therefore be involved in the lead-up to a singularity. They can appear at a singularity but not coalesce with other inflection points or extrema. We therefore need to follow maxima and minima of the component functions, of which X_0 has a finite number and which are, hence, isolated. As component extrema move around during the evolution and cannot increase in number, zeros of the j th component $\partial_s Y^{n,j}$ will occasionally occur at a common parameter value $s_0 \in [0, 1)$ for all $j = 1, \dots, d$. The singularity formed will be a cusp by Proposition 4.7. At such singular points $\partial_s R(Y^n(t_{\text{sing}}))(s_0)$ will experience a U-turn. In the proper coordinates, a (non-degenerate) cusp corresponds to a minimum in the first component and an inflection point in the second (see Proof of 4.7 where it is shown that singularities are asymptotically in a plane). The latter will instantaneously disappear and $\Gamma^n(t_{\text{sing}} + dt)$ will be a smooth curve with at least one less critical point in its components compared to $\Gamma^n(t_{\text{sing}})$. As the inflection point can only have been generated by the merger of extrema, the loss of extremity points as compared to $\Gamma^n(t_{\text{sing}} - dt)$ is at least two. It may happen that a singularity appears at $t \in h\mathbb{N}$, in which case the discussion above still applies. There are therefore at most finitely many singular times during the evolution at each of which at most a finite number of cusps are formed. Notice that degenerate cusps cannot occur since they require vanishing of all derivatives coming into the vertex of the cusp (in the appropriate coordinates), which is only possible for trivial analytic parametrizations. Here we make use of Remark 4.1. \square

Remark 4.12. *The formation of (non degenerate) cusps, which amount to an extremum in a component and an inflection point in another (in the proper coordinates), stems from the merger of two (or more) extrema which give rise to an inflection point. When a maximum and a minimum merge (at a singular time), this corresponds to the evolving curve “shedding” a loop. This phenomenon is depicted in Figure 1.*

Remark 4.13. *The above result shows that inflection points (in any of the components of X^n) appear in tandem with singularities, where maxima and minima merge, and instantaneously disappear. Observe that the main driver of the evolution is diffusion (albeit with varying diffusivity) and that the operator R preserves component minima and maxima in size (while, of course, distorting the shape of the graphs). This means that the flow tries to remove component minima and maxima over time. This can happen without the formation of any singularity or, in the case of coalescence, with the formation of one or more singularities. It follows that there will be an asymptotic number of extremity points as the extinction time (for the limiting flow) is approached. It can be seen that this number is 6 for infinity like shapes, $4n$ for n -fold circular points, and 8 for an Abresch-Langer curve with rotation index 2 and closing up after 3 periods of its curvature function (and hence a perturbation of a doubly covered circle). Figure 7 depicts the evolution of a convoluted curve. It is apparent how the number of extremity points decreases over time with and without singularity formation.*

4.3. The Behavior of Length.

Proposition 4.14. *The length is a continuous non-increasing function of time*

$$L(X^n(t)) \leq L(X^n(\tau)) \leq L(X^n(0)) = L(X_0), \quad t \geq \tau \geq 0, \quad n \in \mathbb{N}.$$

Proof. In the construction of X^n , $X^n(t)$ is obtained either by heat flowing a previous parametrization (with constant but changing time-scale/diffusivity) or by reparametrization. As reparametrization does not change the curve nor its length, it is enough to show that the heat flow of a parametrization with arbitrary diffusivity $\alpha > 0$ exhibits non-increasing length. In other words, let Y satisfy $Y_t = \alpha Y_{ss}$ and consider $L(Y(t)) = \int_0^1 |Y_s(t, \sigma)| d\sigma$. Then

$$\begin{aligned} \frac{d}{dt} L(Y(t)) &= \int_0^1 \frac{Y_s}{|Y_s|} \cdot Y_{st} d\sigma = \alpha \int_0^1 \frac{Y_s \cdot Y_{sss}}{|Y_s|} d\sigma \\ &= -\alpha \int_0^1 \left(\frac{Y_s}{|Y_s|} \right)_s \cdot Y_{ss} d\sigma = -\alpha \int_0^1 \left(\frac{Y_s}{|Y_s|} \right)_s \cdot \left(Y_{ss} - \frac{Y_{ss} \cdot Y_s}{|Y_s|} \frac{Y_s}{|Y_s|} \right) d\sigma \\ &= -\alpha \int_0^1 k(Y) \cdot k(Y) |Y_s|^3 d\sigma \leq 0, \end{aligned} \tag{4.2}$$

where $k(Y)$ is the curvature vector of the curve parametrized by Y . This holds everywhere with the exception of the finitely many singular times away from which continuity follows. At a singular time t_{sing} , $Y^n(t_{sing})$ is a smooth parametrization of a curve with at most finitely many cuspidal points. If $t_{sing} \notin k\mathbb{N}$, then

$$Y^n \in C([t_{sing} - \delta, t_{sing} + \delta], C_\pi^1(I)),$$

for small enough $\delta > 0$ as a solution of $Y_t = \frac{1}{L(X^n(kh))^2} Y_{ss}$ with $Y(t_{sing} - \delta) = Y^n(t_{sing} - \delta)$ and $t_{sing} \pm d \in (kh, (k+1)h)$ and $\int_0^1 |Y_s^n(\cdot, \sigma)| d\sigma$ is therefore continuous at t . If, on the other hand, $t_{sing} = (k+1)h$ for some $k = 0, 1, \dots$, then left continuity follows as above since

$$L(X^n(t)) = L(Y^n(t)) = L(e^{\frac{t-kh}{L^2(X^n(kh))} \partial_{ss}} X^n(kh)), \quad t \in [kh, (k+1)h),$$

and

$$X^n((k+1)h) = R(Y^n((k+1)h)), \quad L(X^n((k+1)h)) = L(Y^n((k+1)h)).$$

For $t > (k+1)h$, we use the fact that $R(Y^n((k+1)h))_s = X_s^n((k+1)h)$ is a continuous function except at mostly finite many points where it has jump discontinuities. In particular, it holds that $X_s^n((k+1)h) \in L_\pi^\infty(I) \subset L_\pi^1(I)$ and then

$$\partial_s e^{\frac{t-(k+1)h}{L^2(X^n(kh))} \partial_{ss}} X^n((k+1)h) = e^{\frac{t-(k+1)h}{L^2(X^n(kh))} \partial_{ss}} X_s^n((k+1)h) \in C([(k+1)h, (k+2)h), L_\pi^1(I)),$$

from which the claim follows. \square

Remark 4.15. *Figure 8 depicts the behavior of length for the flow depicted in Figure 7 where the singular times are clearly visible even in the numerical approximation. The first two occur where the curve loses loops and the last at the extinction time.*

Proposition 4.16. *Setting $L_k = L(X^n(kh))$, $k \geq 1$, it holds that*

$$\begin{cases} L_{k+1} \leq e^{-\frac{h}{L_k^2} 4\pi^2} L_k, & k \geq 0, \\ L_0 = L(X_0). \end{cases} \tag{4.3}$$

Proof. We compute

$$\begin{aligned}
L_{k+1}^2 &= \left(\int_0^1 |Y_s^n((k+1)h, \sigma)| d\sigma \right)^2 \leq \int_0^1 |Y_s^n((k+1)h, \sigma)|^2 d\sigma \\
&= \int_0^1 \sum_{j=1}^d |Y_s^{n,j}((k+1)h, \sigma)|^2 d\sigma = \sum_{j=1}^d \|Y_s^{n,j}((k+1)h)\|_2^2 \\
&\leq e^{-2h \frac{4\pi^2}{L_k^2}} \sum_{j=1}^d \|X_s^{n,j}(kh)\|_2^2 = e^{-2h \frac{4\pi^2}{L_k^2}} \sum_{j=1}^d \int_0^1 |(X_s^{n,j}(kh, \sigma))|^2 d\sigma \\
&= e^{-2h \frac{4\pi^2}{L_k^2}} \int_0^1 \sum_{j=1}^d |(X_s^{n,j}(kh, \sigma))|^2 d\sigma = e^{-2h \frac{4\pi^2}{L_k^2}} L_k^2,
\end{aligned}$$

using the facts that $Y_s^n(t)$ solves $Y_t = \frac{1}{L_k^2} Y_{ss}$ for $t \in (kh, (k+1)h)$ with $Y(kh) = R(Y^n(kh))_s = X_s^n(kh)$ and that $|X_s^n(kh)| = L_k$ as $X^n(kh)$ is normally parametrized. The claim follows. \square

Theorem 4.17. *For any given initial curve $X_0 \in \mathcal{C}(\mathbb{R}^d)$ and any $n \in \mathbb{N}$, it holds that*

$$L(X^n(t)) > 0 \text{ for } t \in [0, \infty),$$

for the evolving family of curves X^n with $X^n(0) = X_0$. For each $n \in \mathbb{N}$, the decrease in length is faster or equal to that of a circle of radius $\frac{L(X_0)}{2\pi}$.

Proof. It follows from careful inspection of the string of inequalities leading to the recursive estimate (4.3), and it will be computed again in Subsection 6.1, that identity actually holds when the initial curve is a circle. Taking its radius to be $\frac{L_0}{2\pi}$, a comparison is obtained for any curve with initial length L_0 . The length is hence strictly decreasing and tends to zero exponentially since the decreasing sequence satisfies

$$L_{k+1} \leq L(t) \leq L_k, \quad t \in [kh, (k+1)h),$$

and $(L_k)_{k \in \mathbb{N}}$ decreases exponentially since

$$\frac{L_k}{L_0} = \prod_{i=1}^k \frac{L_i}{L_{i-1}} \leq \left(e^{-h \frac{4\pi^2}{L_0^2}} \right)^k, \quad k \in \mathbb{N}.$$

The length can, however, not vanish in a finite number of steps since the evolution is driven by linear diffusion on each time interval between hk and $h(k+1)$ with a non trivial (non constant) initial datum. \square

The approximant solution has a infinite extinction time $t_e^n(X_0) = \infty$, regardless of $n \in \mathbb{N}$, and it converges to a point under the effect of diffusion, which drives each component of the position vector to a constant.

Remark 4.18. *Given an initial datum $X_0 \in \mathcal{C}(\mathbb{R}^d)$ and $0 < t < h$, $X_s^n(t)$ is an analytic function of the space variable (regardless of $n \in \mathbb{N}$). It follows that each of its components is either constant or has at most finitely many zeros. In the former case, it must have been a constant component for X_0 also and it will remain constant during the whole evolution. We can therefore assume without loss of generality that the total number of zeros of all components of $X_s^n(h)$ is finite and we may as well assume that this is the case for the initial datum itself.*

Remark 4.19. *It follows from the construction procedure that the length reduction is increasingly pronounced as the total length gets smaller and smaller. This is due to the fact the diffusion coefficient is quadratically inversely proportional to the length of the curve. As the approximation parameter n increases, this coefficient is updated more often and leads to a faster decrease of length. The approximating solution is therefore expected to experience singular points later than any of its limiting curves.*

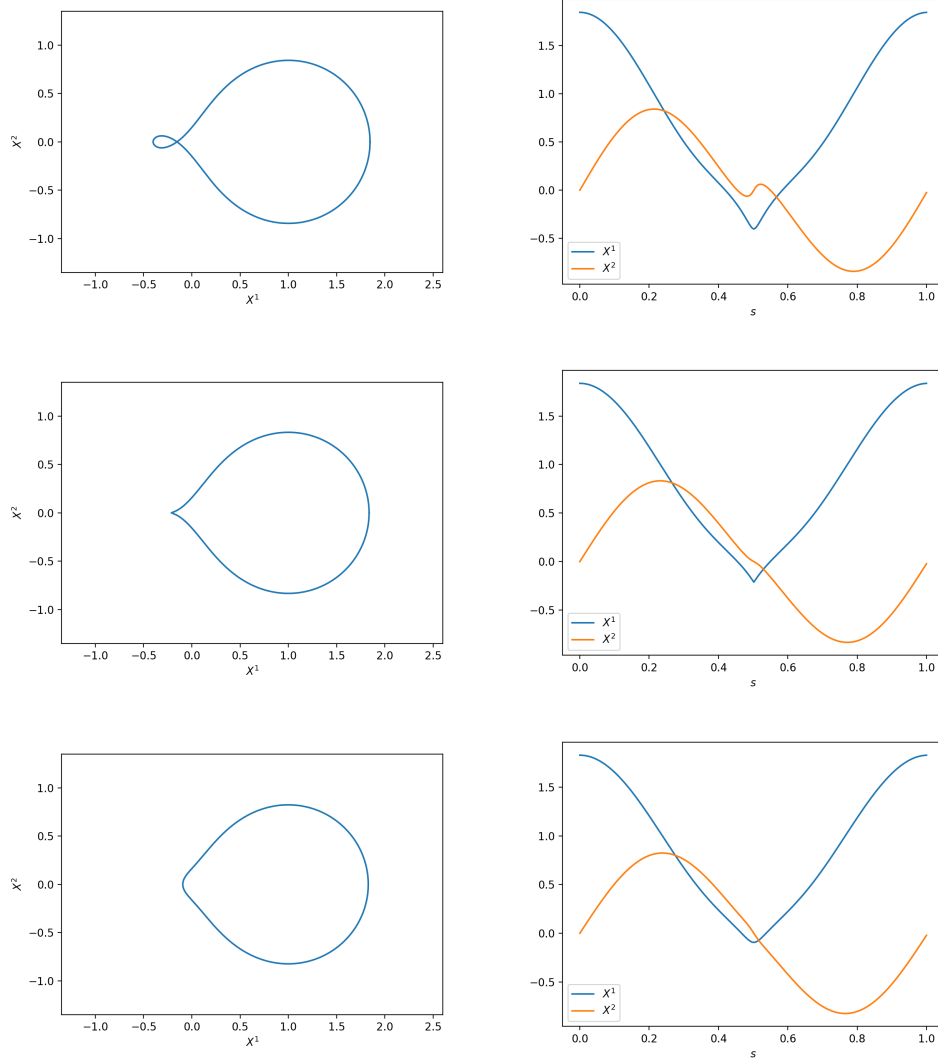


FIGURE 1. Shedding a loop and corresponding singularity. In the first row the evolving curve and its (almost normal) coordinate functions are depicted. The same are shown very close to the singular time in the second row, and after the singularity is regularized by the flow in the third row.

We will show rigorously later that the extinction time $t_e(X_0) < \infty$ for any initial curve (of finite length as considered here). It, however, cannot be excluded in general that $t_e(X_0) = 0$, as will be shown by example below. This can happen when the initial curve is not immersed.

Remark 4.20. The initial datum can be assumed to be essentially parametrized and $X^n(t)$ is always essentially parametrized as either an analytic function or a normal length reparametrization of it.

4.4. The Behavior of Total Curvature. Next we study the behavior of total curvature for the approximant and for smooth solutions of the CSF. For a smooth curve the total absolute curvature is given by

$$\kappa_{tot} = \int_0^L |k| d\bar{s} = \frac{1}{L} \int_0^1 |k| ds,$$

where \bar{s} is arc- and s is normal length.

Proposition 4.21. *Away from singular times, the total curvature along the approximating flow is non-increasing, i.e.*

$$\kappa_{tot}(X^n(t)) \leq \kappa_{tot}(X^n(\tau)) \leq \kappa_{tot}(X^n(0)) = \kappa_{tot}(X_0), \quad 0 \leq \tau \leq t.$$

Proof. The total curvature of a curve is a geometric property that does not depend on the parametrization and it is therefore enough to show that the curve obtained by linear diffusion of a curve's parametrization does not increase total curvature. As the diffusivity is kept piecewise constant for the approximant, we can assume that the diffusivity is 1 and consider a solution of $Y_t = Y_{ss}$ to show the claim. It holds that

$$\kappa_{tot}(Y) = \int_0^1 \left| \left(\frac{Y_s}{|Y_s|} \right)_s \right| ds = \int_0^1 |T_s| ds,$$

where T is unit tangent. Notice that, away from the at most finitely many singularities, $|Y_s| \neq 0$ and T is analytic. As $|T_s| = 0$ at a finite number of parameter values we cannot work with $|T_s|$ directly but replace this quantity by $a_\varepsilon = \sqrt{|T_s|^2 + \varepsilon}$ and compute

$$\frac{d}{dt} \int_0^1 \sqrt{|T_s|^2 + \varepsilon} ds = \int_0^1 \frac{T_s}{a_\varepsilon} \cdot \frac{d}{dt} T_s ds = - \int_0^1 \left(\frac{T_s}{a_\varepsilon} \right)_s \cdot \frac{d}{dt} T ds,$$

and we proceed with the computation of the various terms involved. First notice that

$$\frac{d}{dt} T = \frac{Y_{st}}{|Y_s|} - T \cdot \frac{Y_{st}}{|Y_s|} T = \frac{Y_{sss}}{|Y_s|} - T \cdot \frac{Y_{sss}}{|Y_s|} T =: \frac{Y_{sss}^\perp}{|Y_s|},$$

where the perpendicularity superscript indicates that we are taking the orthogonal projection onto the space perpendicular to T . Next it can be verified that

$$\frac{d}{ds} \left(\frac{T_s}{a_\varepsilon} \right) = \frac{T_{ss}}{a_\varepsilon} - \frac{1}{a_\varepsilon^3} T_s \cdot T_{ss} T_s,$$

taking into consideration the definition of a_ε . It holds that

$$\begin{aligned} T_{ss} &= \left(\frac{Y_{ss}}{|Y_s|} - T \cdot \frac{Y_{ss}}{|Y_s|} T \right)_s = \frac{Y_{sss}}{|Y_s|} - T \cdot \frac{Y_{ss}}{|Y_s|} \frac{Y_{ss}}{|Y_s|} - T_s \cdot \frac{Y_{ss}}{|Y_s|} T - T \cdot \frac{Y_{ss}}{|Y_s|} T_s + \\ &\quad - T \cdot \left(\frac{Y_{sss}}{|Y_s|} - T \cdot \frac{Y_{ss}}{|Y_s|} \frac{Y_{ss}}{|Y_s|} \right) T \\ &= \frac{Y_{sss}^\perp}{|Y_s|} - T \cdot \frac{Y_{ss}}{|Y_s|} \frac{Y_{ss}^\perp}{|Y_s|} - T_s \cdot \frac{Y_{ss}}{|Y_s|} T - T \cdot \frac{Y_{ss}}{|Y_s|} T_s \\ &= \frac{Y_{sss}^\perp}{|Y_s|} - 2T \cdot \frac{Y_{ss}}{|Y_s|} T_s - T_s \cdot \frac{Y_{ss}}{|Y_s|} T. \end{aligned}$$

Then we have that

$$\begin{aligned} \left(\frac{T_s}{a_\varepsilon} \right)_s &= \frac{1}{a_\varepsilon} \left\{ T_{ss} - \frac{T_s}{a_\varepsilon} \cdot T_{ss} \frac{T_s}{a_\varepsilon} \right\} = \frac{1}{a_\varepsilon} \left\{ \frac{Y_{sss}^\perp}{|Y_s|} - 2T \cdot \frac{Y_{ss}}{|Y_s|} T_s - T_s \cdot \frac{Y_{ss}}{|Y_s|} T + \right. \\ &\quad \left. - \frac{T_s}{a_\varepsilon} \cdot \left(\frac{Y_{sss}^\perp}{|Y_s|} - 2T \cdot \frac{Y_{ss}}{|Y_s|} T_s - T_s \cdot \frac{Y_{ss}}{|Y_s|} T \right) \frac{T_s}{a_\varepsilon} \right\} \\ &= \frac{1}{a_\varepsilon} \left\{ \frac{Y_{sss}^\perp}{|Y_s|} - \frac{T_s}{a_\varepsilon} \cdot \frac{Y_{sss}^\perp}{|Y_s|} \frac{T_s}{a_\varepsilon} \right\} - 2 \frac{T \cdot Y_{ss}}{|Y_s|} \frac{T_s}{a_\varepsilon} - \frac{T_s}{a_\varepsilon} \cdot \frac{Y_{ss}}{|Y_s|} T \\ &\quad + 2 \frac{T_s}{a_\varepsilon} \cdot \frac{T_s}{a_\varepsilon} \frac{T \cdot Y_{ss}}{|Y_s|} \frac{T_s}{a_\varepsilon} + \frac{T_s}{a_\varepsilon} \cdot T \frac{T_s}{a_\varepsilon} \cdot \frac{Y_{ss}}{|Y_s|} \frac{T_s}{a_\varepsilon} \\ &= \frac{1}{a_\varepsilon} \left\{ \frac{Y_{sss}^\perp}{|Y_s|} - \frac{T_s}{a_\varepsilon} \cdot \frac{Y_{sss}^\perp}{|Y_s|} \frac{T_s}{a_\varepsilon} \right\} - 2 \frac{T \cdot Y_{ss}}{|Y_s|} \frac{T_s}{a_\varepsilon} \left(1 - \frac{T_s}{a_\varepsilon} \cdot \frac{T_s}{a_\varepsilon} \right) - \frac{T_s}{a_\varepsilon} \cdot \frac{Y_{ss}}{|Y_s|} T \end{aligned}$$

Combining everything we compute

$$\left(\frac{T_s}{a_\varepsilon}\right)_s \cdot \frac{d}{dt}T = \frac{1}{a_\varepsilon} \left\{ \frac{|Y_{sss}^\perp|^2}{|Y_s|^2} - \left(\frac{T_s}{a_\varepsilon} \cdot \frac{Y_{sss}^\perp}{|Y_s|}\right)^2 \right\} - 2 \frac{T \cdot Y_{ss}}{|Y_s|} \frac{T_s}{a_\varepsilon} \cdot \frac{Y_{sss}^\perp}{|Y_s|} \left(1 - \frac{T_s}{a_\varepsilon} \cdot \frac{T_s}{a_\varepsilon}\right) = I - II$$

In order gain insight into the two terms above we write $u = \frac{Y_{ss}}{|Y_s|}$ and $v = \frac{Y_{sss}}{|Y_s|}$ and work in an orthonormal basis starting with $e_1 = T$, $e_2 = \frac{T_s}{|T_s|}$. Notice that such a basis exists almost everywhere since T_s can only vanish finitely many times. Then term I reads

$$\frac{1}{a_\varepsilon} (v_2^2 + \dots + v_d^2 - \frac{a_0^2}{a_\varepsilon^2} v_2^2) \geq 0$$

since $|T_s| = a_0 \leq a_\varepsilon$. For II we have

$$II = -2u_1 \frac{a_0}{a_\varepsilon} v_2 \left(1 - \frac{a_0^2}{a_\varepsilon^2}\right) \longrightarrow 0 \quad (\varepsilon \rightarrow 0).$$

By Lebesgue's dominated convergence theorem we finally arrive at

$$\int_0^1 |T_s|(t) ds - \int_0^1 |T_s|(\tau) ds \leq 0 \text{ for } t \geq \tau,$$

where t and τ are in between singular times. Indeed

$$\int_0^1 \sqrt{|T_s|^2(t) + \varepsilon} ds - \int_0^1 \sqrt{|T_s|^2(\tau) + \varepsilon} ds = - \int_\tau^t \int_0^1 \{I + II\} \leq - \int_\tau^t \int_0^1 II,$$

and the claim follows from the almost everywhere convergence and everywhere boundedness of II , as well as the convergence of the terms on the left as $\varepsilon \rightarrow 0$. \square

Proposition 4.22. *The total curvature is non-increasing for any smooth solution of the CSF in any space dimension.*

Proof. We borrow the idea of the proof from [2] where the case of 3D space curves is considered. For this proof we denote the arclength parameter by s instead of \bar{s} . If X solves the CSF and is smooth, then

$$\kappa(X) = |k(X)| = |X_{ss}|.$$

First we derive an equation for $|X_{ss}|^2$ and then deal with the total curvature. It holds that

$$\begin{aligned} \frac{d}{dt}|X_{ss}|^2 &= 2 \frac{d}{dt} \frac{d}{ds} \frac{d}{ds} X \cdot X_{ss} = 2 \left[\frac{d}{ds} \frac{d}{dt} \frac{d}{ds} X + |X_{ss}|^2 X_{ss} \right] \cdot X_{ss} \\ &= 2 \left[\frac{d^2}{ds^2} \frac{d}{dt} X + \frac{d}{ds} (|X_{ss}|^2 X_s) + |X_{ss}|^2 X_{ss} \right] \cdot X_{ss} \\ &= 2 \frac{d^2}{ds^2} X_{ss} \cdot X_{ss} + 2|X_{ss}|^4 + 4(X_{sss} \cdot X_{ss})(X_s \cdot X_{ss}) \\ &= 2 \frac{d^2}{ds^2} X_{ss} \cdot X_{ss} + 2|X_{ss}|^4 \end{aligned}$$

since $\frac{d}{dt} \frac{d}{ds} = \frac{d}{ds} \frac{d}{dt} + \kappa^2 \frac{d}{ds}$ and $X_{ss} \cdot X_s \equiv 0$. Next we use that

$$\frac{d^2}{ds^2} (X_{ss} \cdot X_{ss}) = 2 \frac{d^2}{ds^2} X_{ss} \cdot X_{ss} + 2X_{sss} \cdot X_{sss},$$

to see that

$$\frac{d}{dt}|X_{ss}|^2 = \frac{d^2}{ds^2}|X_{ss}|^2 - 2X_{sss} \cdot X_{sss} + 2|X_{ss}|^4.$$

In order to deal with $|X_{ss}|$ we use a “regularization” that Altschuler attributes to Hamilton in [2] and derive first an equation for $\kappa_\varepsilon = \sqrt{|X_{ss}|^2 + \varepsilon}$. It holds that

$$\frac{d}{dt}\kappa_\varepsilon = \frac{1}{\kappa_\varepsilon} \frac{d}{dt}|X_{ss}|^2 = \frac{1}{\kappa_\varepsilon} \left[\frac{1}{2} \frac{d^2}{ds^2}|X_{ss}|^2 - X_{sss} \cdot X_{sss} + |X_{ss}|^4 \right],$$

and we compute

$$\begin{aligned} \frac{d^2}{ds^2}\kappa_\varepsilon &= \frac{d}{ds} \left(\frac{1}{\kappa_\varepsilon} X_{sss} \cdot X_{ss} \right) = -\frac{1}{\kappa_\varepsilon^3} (X_{sss} \cdot X_{ss})^2 + \frac{1}{\kappa_\varepsilon} (X_{ssss} \cdot X_{ss} + X_{sss} \cdot X_{sss}) \\ &= -\frac{1}{\kappa_\varepsilon^3} (X_{sss} \cdot X_{ss})^2 + \frac{1}{2\kappa_\varepsilon} \frac{d^2}{ds^2}|X_{ss}|^2, \end{aligned}$$

thus arriving at

$$\frac{d}{dt}\kappa_\varepsilon = \frac{d^2}{ds^2}\kappa_\varepsilon + \frac{1}{\kappa_\varepsilon^3} (X_{sss} \cdot X_{ss})^2 - \frac{1}{\kappa_\varepsilon} |X_{sss}|^2 + \frac{|X_{ss}|^4}{\kappa_\varepsilon}.$$

Finally we compute

$$\frac{d}{dt} \int \kappa_\varepsilon ds = \int \left(\frac{d}{dt}\kappa_\varepsilon - |X_{ss}|^2 \kappa_\varepsilon \right) ds$$

and exploit the fact that

$$\frac{|X_{ss}|^4}{\kappa_\varepsilon} \leq |X_{ss}|^2 \kappa_\varepsilon \text{ and } \frac{1}{\kappa_\varepsilon^3} (X_{sss} \cdot X_{ss})^2 \leq \frac{|X_{sss}|^2}{\kappa_\varepsilon},$$

as follows from $|X_{ss}| \leq \kappa_\varepsilon$, to obtain that

$$\frac{d}{dt} \int \kappa_\varepsilon ds \leq 0,$$

which yields the claim in the limit as $\varepsilon \rightarrow 0$. \square

Remark 4.23. In [2] the Frenet-Serret formulæ for space curves ($d = 3$) are used and the decay of the total curvature is measured in terms of the curvature and of the torsion τ to give the stronger estimate

$$\frac{d}{dt} \int |k| ds \leq - \int \tau^2 |k| ds.$$

This estimate is then used in the same paper to show that singularity formation for space curves is a planar phenomenon.

Remark 4.24. During the flow, some curvature can occasionally (a finite number of times) concentrate (blow up in a controlled way) at finitely many singular points but, as a measure, it is always defined. In this sense curvature never blows up during the evolution (and, in the limit as $n \rightarrow \infty$, blows up only once and this happens at the extinction time).

Remark 4.25. When the evolving curve develops one or more of its finite singularities, it is in the form of a cusp. In such a situation the total (angular) curvature has a jump (in time) where it decreases instantaneously by π for each cusp that is formed. Notice also that, thanks to Proposition 4.7, the (spatial) singularities are asymptotically two dimensional (regular cusps) or one dimensional (degenerate cusps).

5. EXISTENCE OF A LIMITING FLOW

Theorem 5.1. Let $X_0 \in \mathcal{IC}_e(\mathbb{R}^d)$ be given such that $\kappa_{\text{tot}}(\Gamma_0) < \infty$. Then the sequence $(X^n)_{n \in \mathbb{N}}$ converges uniformly to a solution $X : [0, \infty) \rightarrow \mathbb{R}^d$ of the CSF (2.4). The solution X has finite extinction time $t_e(X_0)$, which is bounded above by the extinction time of a circle of radius $\frac{L(X_0)}{2\pi}$.

If the initial datum has a finite number of extremity points, the limit has at most a finite number of singular times away from which it is smooth (in space and time) and hence satisfies the equation in the classical sense.

Proof. We assume that $t_e(X_0) > 0$ because in the degenerate situation that $t_e(X_0) = 0$ there is nothing to prove. When $d = 2$ this is always the case as soon as X_0 has a loop that contains a circle.

(i) Propositions 4.2 and 4.21 ensure that

$$X^n \in W_\infty^1([0, \infty), E_0) \cap L^\infty([0, \infty), E_1),$$

with a bound on the norm which is independent of $n \in \mathbb{N}$. Here we set

$$E_0 = \mathcal{M}_\pi(I) \text{ and } E_1 = \{Y \in W_{\infty, \pi}^1(I) \mid Y_s \in \text{BV}_\pi(I)\}.$$

Observing that $W_{p', \pi}^s(I) \xrightarrow{d} C_\pi(I)$ for $s > 1/p'$ and $p' \in (1, \infty)$, we infer the validity of the embedding $E_0 = \mathcal{M}_\pi(I) \hookrightarrow W_{p, \pi}^{-s}(I) =: F_0$. Notice that $E_1 \hookrightarrow W_{p, \pi}^1(I) =: F_1$ for every $p > 1$. Then

$$W_\infty^1([0, \infty), E_0) \cap L^\infty([0, \infty), E_1) \hookrightarrow W_\infty^1([0, \infty), F_0) \cap L^\infty([0, \infty), F_1). \quad (5.1)$$

Using the real interpolation functor we see that

$$(F_0, F_1)_{\theta, p} = W_{p, \pi}^{\theta-s(1-\theta)}(I), \quad \theta \in (0, 1),$$

and, consequently that

$$W_\infty^1([0, \infty), E_0) \cap L^\infty([0, \infty), E_1) \hookrightarrow C^{1-\theta}([0, \infty), W_{p, \pi}^{\theta-s(1-\theta)}(I)),$$

using (5.1), the interpolation inequality for $(F_0, F_1)_{\theta, p}$, and the fundamental theorem of calculus. By choosing $1 > \theta > \frac{1+s-\delta}{1+s}$, it can be achieved that $\theta - s(1-\theta) > 1-\delta$ for any small $\delta > 0$. Thus, for any $\delta \in (0, 1)$, there is $r > 0$ (small) such that

$$X^n \in C^r([0, \infty), W_{p, \pi}^{1-\delta}(I))$$

with a bound that is uniform in $n \in \mathbb{N}$. As the first embedding below is compact,

$$C^r([0, T], W_{p, \pi}^{1-\delta}(I)) \hookrightarrow C^{\tilde{r}}([0, T], W_{p, \pi}^{1-\tilde{\delta}}(I)) \hookrightarrow C^\rho([0, T] \times I), \quad \tilde{r} < r, \tilde{\delta} > \delta,$$

and the second is valid for $\rho > 0$ small enough, it is possible to extract a subsequence that converges in the second space for any $T > 0$ to a limiting function X that is an element of the first space and for which convergence is uniform in space and time due the second embedding. Notice that $X(T, \cdot)$ must have finite length by lower semicontinuity of length. If $L(X(T, \cdot)) > 0$, then, given $0 < \varepsilon < L(X(T, \cdot))$, it is possible to find $m \in \mathbb{N}$ and a partition $(s_j^m)_{j=0}^{m-1}$ of parameter space such that

$$L(X(T, \cdot)) - \frac{\varepsilon}{2} \leq \sum_{j=0}^{m-1} |X(T, s_{(j+1) \bmod m}) - X(T, s_j)|,$$

since the length of $X(T, \cdot)$ is the supremum of the above expression over all partitions. Due to the uniform convergence of $X^n(T, \cdot)$, $N \in \mathbb{N}$ can be found such that

$$L(X^n(T, \cdot)) \geq \sum_{j=0}^{m-1} |X^n(T, s_{(j+1) \bmod m}) - X^n(T, s_j)| \geq L(X(T)) - \varepsilon \text{ for } n \geq N. \quad (5.2)$$

(ii) The approximants X^n are smooth for $0 < t < t_{1, \text{sing}}^n(X_0)$ with respect to the spatial variable due to the smoothing properties of the heat equation and with respect of the time variable with the exception of the discrete time of juncture. Here $t_{1, \text{sing}}^n$ is the first (if any) singular time in their evolution, and

$$t_{1, \text{sing}}^\infty = \liminf_{n \rightarrow \infty} t_{1, \text{sing}}^n(X_0) > 0,$$

since isolated extremal points cannot merge instantaneously by local well-posedness of the CSF. As a consequence $|X_s^n(t, \cdot)|$ is bounded away from zero independly of n and the reparametrizations at juncture times ($t = kh$, $k \in \mathbb{N}$) preserve the regularity (as they does not change the curve¹). The bounding constant for spatial norms depends only on the initial datum X_0 on any compact subinterval

¹It is enough to exclude the possibility of a smoothly parametrized singular curve.

of $(0, t_{1,sing}^\infty)$. As with time, the dependence is at most Lipschitz due to the junctures. Thus, for any compact subinterval J of $(0, t_{1,sing}^\infty)$, we have that X^n is bounded in $C^{1-}(J, C_\pi^{2+\varepsilon}(I))$. It is therefore possible to go to limit (along a further subsequence) in

$$X_t^n(t) = \frac{1}{L^2(X^n(k_th))} \partial_{ss} e^{\frac{t-k_th}{L^2(X^n(k_th))}} \partial_{ss} R(X^n(k_th)), \quad t \in [k_th, (k_t+1)h),$$

to obtain that $X_t = \frac{1}{L^2(X)} \partial_{ss} R(X)$ for $t \in (0, t_{1,sing}^\infty)$ as $k_th \rightarrow t$ as $h \rightarrow 0$ since X_t can only be the limit of the right-hand-side by closure. Notice that, while the time derivative experiences jumps at the juncture time for X^n , these gaps closes up in the limit as left and right limits coincide in the limit due to the strong spatial convergence and time continuity. It follows that X is a smooth solution of the CSF on an open interval. It may develop one or more singularities at some time $t_{1,sing} > 0$ but, even then, we can use Proposition 4.22 to see that it remains a finite length curve of finite total curvature in the limit. The limiting curve at the singular time is given by $X(t_{1,sing})$ since X exists for all times. It is possible that $t_{1,sing} = t_e(X_0)$.

(iii) If $t_{1,sing} < t_e(X_0)$, it follows from (ii) that $X(t_{1,sing})$ is a curve of finite total curvature and it clearly still has a finite number of extremity points. We can therefore argue as above with $X(t_{1,sing})$ as a new initial datum and obtain that X is a smooth solution of the CSF for $t \in (t_{1,sing}, t_{2,sing})$ and some $t_{2,sing} > t_{1,sing}$. Again, if $t_{2,sing} < t_e(X_0)$, the argument can be repeated. We end up with a solution X that is smooth up to a finite number of singular times where it exhibits a finite number of singular points where a non-trivial amount of total curvature concentrates (more precisely total curvature has a density with a singular component concentrated at the singular points). When $t_e(X_0)$ is reached, the curvature truly blows up as the length vanishes (with total curvature settling on a limit).

(iv) We already know that the length of X depends continuously on time and it is approached uniformly by $L(X^n)$ on compact time intervals away from singular times. Using Proposition 4.3 it is seen that

$$L_{k_t+dt} \leq e^{-4\pi^2 h (\frac{1}{L_{k_t+dt}^2} + \dots + \frac{1}{L_{k_t}^2})} L_{k_t}$$

where $t \in [k_th, (k_t+1)h)$ for any t , and where $dt > 0$. Notice that L_k also depends on $n \in \mathbb{N}$ but we omit the n dependence for readability. Letting $n \rightarrow \infty$ ($h \rightarrow 0$), we obtain that

$$\frac{L(t+dt) - L(t)}{dt} \leq \frac{e^{-4\pi^2 \int_t^{t+dt} \frac{1}{L^2(\tau)} d\tau} - 1}{dt} L(t), \quad t > 0.$$

As this is valid regardless of the choice of $t > 0$ and $dt > 0$ as long as $L(t+dt) > 0$ we let $dt \rightarrow 0$ to see that

$$\limsup_{dt \rightarrow 0} \frac{L(t+dt) - L(t)}{dt} \leq -\frac{4\pi^2}{L(t)}.$$

As the limiting curve flow has at most countably many points of discontinuity (finitely many in fact), the above limit coincides with the actual derivative a.e. and, integrating, we see that

$$L(t) \leq \sqrt{L_0^2 - 8\pi^2 t},$$

for as long as the length remains positive. Thus the solution becomes a point in finite time $t_e(X_0) < \infty$. This extinction time is at most the time it takes a circle of radius $\frac{L_0}{2\pi}$ to shrink to a point, which is precisely given by the right-hand expression in the inequality as is explicitly computed in the next section. \square

Remark 5.2. *The construction of a solution works also for non-immersed initial data in $C_e(\mathbb{R}^d)$. This is a case in which it is possible that $t_e(X_0) = 0$. We conjecture that this happens only for deformations*

of doubly (or multiply) covered segments (including “curved” ones). Such curves, in the doubly covered case, are characterized by the symmetry given by

$$X_0\left(\frac{1}{2} + s\right) = X_0\left(\frac{1}{2} - s\right), \quad s \in [0, 1],$$

of their normal parametrization, i.e. curves that start in one (end)point, reach another, and return along the same path to the starting point. The case of a doubly covered segment is discussed in the next section.

Remark 5.3. When $d = 2$, using the same proof found in the paper [6] by Angenent based on the maximum principle, one obtains unique local existence in time for the solution to the CSF to any initial datum $X_0 \in \mathcal{IC}_e(\mathbb{R}^d)$ for which $\partial_{ss}R(X_0)$ is a Radon measure or, more specially, has a singular part consisting of Dirac measures only. Uniqueness in general dimensions holds in as far it does for local in time classical solutions with initial data of the regularity considered here.

Remark 5.4. The solution construction procedure highlights the fact that the singularities incurred during the flow are due to diffusion and not to the nonlinear nature of the equation. The reparametrization operator R does not engender any geometric singularity and the decreasing length only modulates the diffusive strength causing extinction to occur in finite rather than infinite time. Diffusion is also responsible for driving each component of $X^n(t)$ to a constant, i.e. for eventual convergence to a point independently of the initial datum.

Proposition 5.5. At a singularity time $t_{\text{sing}} \leq t_e(X_0)$, $X(t_{\text{sing}})(I)$ either is a point (if $t_{\text{sing}} = t_e(X_0)$) or it possesses one or more cuspidal points. A cusp is formed when the evolving curve loses a loop which shrinks to the corresponding cuspidal point.

Remark 5.6. When $d = 2$, a smooth embedded curve does consist of a single loop and X^n does not experience any singularity during its entire evolution and, in the limit, until its extinction time.

Proof. For any fixed n , a (cusp) singularity can only form by the merger of extrema, i.e. from the disappearance of a loop. Thus no singularity can form since the initial curve consists of a single loop and its disappearance would signify collapsing to a point in finite time. Taking a time $0 < t < t_e(X^0)$, any finite regularity space norm of X^n and its Lipschitz time norm can be bounded on $[0, t] \times I$ since $|Y_s^n|$ is never zero and thus bounded away from zero on $[0, t] \times I$ thanks to (5.2) and $L(X(t, \cdot)) > 0$. Thus, on the same interval, $X = \lim_{n \rightarrow \infty} X^n$ is a classical solution (as argued in the proof of Theorem 5.1) and does not develop singularities. As $t < t_e(X^0)$ is arbitrary, the claim follows. \square

6. SPECIAL SOLUTIONS

Next we study the constructed solution to the CSF in three special cases: circles, a doubly covered segment, and a class of figure infinity shapes (also known as figure eight curves in the literature).

6.1. Circles. We already know that the only self-similarly evolving curves that remain normally parametrized for all times are circles (possibly multiply covered) in a plane. It is enough to consider the simply covered case where we can assume without loss of generality that

$$X_0 = (\cos(2\pi s), \sin(2\pi s), 0, \dots, 0), \quad s \in [0, 1],$$

so that the problem can be formulated in a plane and the additional coordinates neglected. Clearly $R(X_0) = X_0$ so that

$$X^n(h) = e^{\frac{h}{L_0^2} \partial_{ss}} X_0 = e^{-\frac{h}{4\pi^2} 4\pi^2} X_0 = e^{-h} X_0 \quad \text{for } L_0 = 2\pi,$$

and similarly

$$X^n(2h) = e^{\frac{h}{L_1^2} \partial_{ss}} X^n(h) = e^{-\frac{h}{e^{-2h}}} X^n(h) \quad \text{for } L_1 = L(X^n(h)) = 2\pi e^{-h},$$

so that the recursion

$$X^n((k+1)h) = e^{-\frac{h}{L_k^2} \partial_{ss}} X^n(kh) \text{ for } L_k = L(X^n(kh)), k \geq 2,$$

is obtained. It is, however, clearly enough to follow the length as the shape does not change, in which case we arrive at

$$\begin{cases} L_{k+1} = e^{-\frac{4\pi^2 h}{L_k^2}} L_k, & k \geq 0 \\ L_0 = 2\pi. \end{cases}$$

Then

$$L_k = e^{-\frac{t}{n} \frac{4\pi^2}{L_{k-1}^2} - \dots - \frac{t}{n} \frac{4\pi^2}{L_0^2}},$$

which is a discretization of

$$L(t) = e^{-\int_0^t \frac{4\pi^2}{L^2(\tau)} d\tau} L_0,$$

and thus of the ODE

$$\dot{L}(t) = -\frac{4\pi^2}{L^2(t)} e^{-\int_0^t \frac{4\pi^2}{L^2(\tau)} d\tau} L_0 = -\frac{4\pi^2}{L(t)}, \quad L(0) = L_0,$$

which we know to be the exact evolution of the length under the CSF in this case, as follows from (3.1), for instance.

7. DOUBLY COVERED SEGMENTS

Again we can assume to be working in the plane and start with a smooth parametrization of the doubly covered segment $[-\frac{L_0}{4}, \frac{L_0}{4}]$, which has length L_0 , given by

$$X_0(r) = \left(\frac{L_0}{4} \cos(2\pi r), 0\right), \quad r \in [0, 1).$$

We parametrize in this way to underscore the connection to the first non-trivial mode of $-\partial_{ss}$ and to suggest that its evolution may be thought of as a degenerate self-similar flow. It holds that

$$R(X_0)(s) = \begin{cases} (-\frac{L_0}{4} + L_0 s, 0), & s \in [0, \frac{1}{2}), \\ (\frac{3}{4}L_0 - L_0 s, 0), & s \in [\frac{1}{2}, 1). \end{cases}$$

Notice that this curve has infinitely many extremity points and does therefore not satisfy the assumption made earlier, if considering it a curve in the plane or higher dimensional space. Confined to the one dimensional line it spans, however, it has a finite number of extremity points. The construction of the solution can be carried out. As computed previously, we have that

$$\partial_{ss} R(X_0) = (2L_0(\delta_0 - \delta_{\frac{1}{2}}), 0).$$

In order to obtain $e^{\frac{h}{L_0^2} \partial_{ss}} R(X_0)$ we solve

$$\begin{cases} Y_t = \frac{1}{L_0^2} Y_{ss}, \\ Y(0) = 2L_0 \partial_{ss}^{-1} (\delta_0 - \delta_{\frac{1}{2}}), \end{cases}$$

where the inverse ∂_{ss}^{-1} is taken in the space of mean zero functions. It follows that

$$\widehat{Y(0)}_\ell = \frac{2L_0}{4\pi^2 \ell^2} (e^{-2\pi i \ell \frac{1}{2}} - e^{-2\pi i \ell 0}) = \frac{L_0}{2\pi^2 \ell^2} ((-1)^\ell - 1) = \begin{cases} 0, & \ell \text{ even}, \\ -\frac{L_0}{\pi^2 \ell^2}, & \ell \text{ odd}, \end{cases}$$

so that

$$Y^n(h) = - \sum_{\ell \text{ odd}} \frac{L_0}{\pi^2 \ell^2} e^{-\frac{4\pi^2}{L_0^2} \ell^2 h} e^{2\pi i \ell s},$$

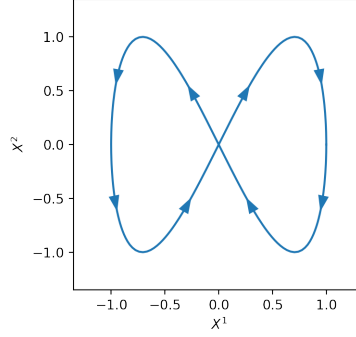


FIGURE 2. A symmetric figure infinity (or figure eight).

and then

$$L_1 = L_0 \sum_{\ell \text{ odd}} \frac{2}{\pi^2 \ell^2} e^{-\frac{4\pi^2}{L_0^2} \ell^2 h} \leq L_0 \frac{\pi^2}{8} \frac{2}{\pi^2} = \frac{1}{4} L_0,$$

using the fact that $\sum_{\ell \text{ odd}} \frac{1}{\ell^2} = \frac{\pi^2}{8}$. This remains true in any step of the approximate evolution and it therefore holds that

$$L_n(t) = L_n \leq \frac{1}{4^n} L_0 \rightarrow 0 \text{ as } n \rightarrow \infty,$$

for $h = \frac{t}{n}$. Thus the limiting solution of the curve shortening flow instantaneously collapses to a point, i.e.

$$X(t) = \begin{cases} X_0, & t = 0, \\ \{(0, 0)\}, & t > 0. \end{cases}$$

Remark 7.1. A doubly covered segment can be viewed as the limit of an ellipse with vanishing aspect ratio such as the one satisfying

$$\left(\frac{2x}{L_0}\right)^2 + \left(\frac{2y}{\varepsilon}\right)^2 = 1.$$

As the area of this simple curve is reduced at the constant rate 2π by the CSF, it limits to a circular point at $t_e = \frac{L_0^2}{8\varepsilon}$. The doubly covered segment inside shrinks faster than the ellipse does, regardless of $\varepsilon > 0$. It must therefore vanish instantaneously in line with what we proved above.

Remark 7.2. A doubly covered segment can also be thought of as a degenerate loop. We conjecture that any smooth initial datum with added “hairs”, i.e. with added degenerate loops, instantaneously absorbs all of them and evolves just as if it did not have any hair. Numerical experiments (not shown) and the behavior of the doubly covered segment support this conjecture.

8. THE FIGURE INFINITY SHAPE

Consider any closed curve with the symmetries of the planar shape ∞ with the origin in the self-intersection point and that is specularly symmetric with respect to both axes. See Figure 2. Such a shape will have a parametrization X_0 that we can assume to be normal and to start at the extreme point to the right. We shall also assume that the curve self-intersects at the origin transversally (as opposed to the corresponding “almost embedded singular curve” which merely self-touches in the origin). An example of a curve with the desired properties but not normally parametrized is given by

$$X_0 = \left(\cos\left(r - \frac{\pi}{2}\right), \sin(\pi - 2r)\right), \quad r \in [0, 2\pi).$$

Notice that the curve starts at the origin and loops back to it visiting the first and last quadrant

before entering the second quadrant and looping back to the origin through the third. The imposed symmetries imply that

$$X_0^1\left(\frac{k}{4} + s\right) = (-1)^k X_0^1\left(\frac{k}{4} - s\right) \text{ for } s \in [0, 1) \text{ and } k = 1, \dots, 4, \quad (8.1)$$

and that

$$X_0^2\left(\frac{k}{8} + s\right) = (-1)^{k+1} X_0^2\left(\frac{k}{8} - s\right) \text{ for } s \in [0, 1) \text{ and } k = 1, \dots, 8. \quad (8.2)$$

These symmetries are preserved for all times along any approximant $X^n(t)$ by the unique solvability of the heat equation and by the fact that they are clearly preserved when reparametrizing by an application of R in the sense that, while formulated in terms of the normal parametrization, they are geometric in nature, i.e. symmetries of the image set. As n is arbitrary the limiting CSF solution X will also enjoy these symmetries due to uniform convergence. This means that the signed enclosed area always vanishes (and hence is independent of the direction of the parametrization) since it does for X_0 as a consequence of the shapes' symmetries. This already excludes that this curve converge to a circular point, which has positive enclosed area that only vanishes at the extinction time. Next observe that the symmetries of the component functions X^1 and X^2 also imply that, for every $t > 0$,

$$\begin{aligned} \int_0^1 X^1(t, s) \sin(2\pi s) ds &= 0, \quad \int_0^1 X^1(t, s) \cos(2\pi s) ds \neq 0 \text{ for every } t \in [0, t_e), \\ \int_0^1 X^2(t, s) \varphi(s) ds &= 0 \text{ for every } t \in [0, t_e) \text{ and } \varphi = \cos(2\pi \cdot), \sin(2\pi \cdot), \\ \int_0^1 X^2(t, s) \sin(4\pi s) ds &\neq 0 \text{ for every } t \in [0, t_e), \end{aligned}$$

Notice how the first component will have a non-zero first cosine mode, while it will vanish for the second component. For the latter, the second sine mode will not vanish. This means that, for all approximants, the first component will decay at an exponential rate of at least $-\frac{4\pi^2}{L^2}$ where L is the appropriate length for the corresponding time interval. The second component, however, will decay with an exponential rate of $-\frac{16\pi^2}{L^2}$ at least. It follows that, independently of the approximant, the aspect ratio $\frac{\text{diam}_x(X^n(t))}{\text{diam}_y(X^n(t))}$ of the evolving shape will converge to zero as the extinction time is approached.

Theorem 8.1. *Let X_0 be an infinity shape with the above symmetries and a transversal self-intersection. Then it will not limit to a circular point, but rather to a zero aspect ratio doubly covered segment-like point.*

Proof. First observe that the symmetries assumed on X_0 translate into symmetries of the normal and curvature vectors and thus any solution of the CSF (as well as of the approximating flow) will preserve them. A first consequence of these symmetries is that the evolving curve will bound a region of vanishing signed area centered in the origin. Indeed, it follows from

$$Y\left(\frac{1}{2} + s\right) = -Y\left(\frac{1}{2} - s\right), \quad s \in [0, \frac{1}{2}),$$

that

$$\begin{aligned}
\int_{\Gamma} x^1 dx^2 &= \int_0^{\frac{1}{2}} Y^1(s) \frac{d}{ds} Y^2(s) ds + \int_{\frac{1}{2}}^1 Y^1(s) \frac{d}{ds} Y^2(s) ds \\
&= \int_0^{\frac{1}{2}} Y^1(s) \frac{d}{ds} Y^2(s) ds + \int_0^{\frac{1}{2}} Y^1\left(\frac{1}{2} + s\right) \frac{d}{ds} Y^2\left(\frac{1}{2} + s\right) ds \\
&= \int_0^{\frac{1}{2}} Y^1(s) \frac{d}{ds} Y^2(s) ds - \int_0^{\frac{1}{2}} Y^1\left(\frac{1}{2} - s\right) \frac{d}{ds} Y^2\left(\frac{1}{2} - s\right) ds \\
&= \int_0^{\frac{1}{2}} Y^1(s) \frac{d}{ds} Y^2(s) ds - \int_0^{\frac{1}{2}} Y^1(s) \frac{d}{ds} Y^2(s) ds = 0,
\end{aligned}$$

where $\Gamma = Y([0, 1])$ is any curve with the discussed symmetries. Thus the signed area indeed vanishes along the (approximate) CSF flow and this alone excludes the possibility that the curve shrinks to a round point. If that were the case, the area would have to be positive for a non-empty interval of time before extinction. Now notice that

$$\begin{aligned}
\cos\left(2\pi\left(\frac{k}{4} + s\right)\right) &= (-1)^k \cos\left(2\pi\left(\frac{k}{4} - s\right)\right) \\
\sin\left(2\pi\left(\frac{k}{4} + s\right)\right) &= (-1)^{k+1} \sin\left(2\pi\left(\frac{k}{4} - s\right)\right).
\end{aligned}$$

Using (8.1), we see that

$$\begin{aligned}
\int_0^1 X_0^1(s) \sin(2\pi s) ds &= \sum_{k=0}^3 \int_{\frac{k}{4}}^{\frac{k+1}{4}} X_0^1(s) \sin(2\pi s) ds = \sum_{k=0}^3 \int_0^{\frac{1}{4}} X_0^1\left(\frac{k}{4} + s\right) \sin\left(2\pi\left(\frac{k}{4} + s\right)\right) ds \\
&= (-1)^{2k+1} \sum_{k=0}^3 \int_0^{\frac{1}{4}} X_0^1\left(\frac{k}{4} - s\right) \sin\left(2\pi\left(\frac{k}{4} - s\right)\right) ds \\
&= \sum_{k=0}^3 \int_{\frac{1}{4}}^0 X_0^1\left(\frac{k}{4} + s\right) \sin\left(2\pi\left(\frac{k}{4} + s\right)\right) ds \\
&= - \int_0^1 X_0^1(s) \sin(2\pi s) ds
\end{aligned}$$

and thus

$$\int_0^1 X_0^1(s) \sin(2\pi s) ds = 0.$$

Next observe that

$$X_0^1(s) > 0 \text{ on } \left(0, \frac{1}{2}\right) \text{ and } X_0^1(s) < 0 \text{ on } \left(\frac{1}{2}, 1\right),$$

and that

$$\cos(2\pi s) > 0 \text{ on } \left(0, \frac{1}{2}\right) \text{ and } \cos(2\pi s) < 0 \text{ on } \left(\frac{1}{2}, 1\right).$$

It follows that

$$\int_0^1 X^1(t, s) \cos(2\pi s) ds = \int_0^{\frac{1}{2}} X^1(t, s) \cos(2\pi s) ds + \int_{\frac{1}{2}}^1 X^1(t, s) \cos(2\pi s) ds > 0.$$

As for X_0^2 we have that

$$\begin{aligned}
\int_0^1 X_0^2(s) \sin(2\pi s) ds &= \sum_{k=0}^3 \int_{\frac{k}{4}}^{\frac{k+1}{4}} X_0^2(s) \sin(2\pi s) ds = \sum_{k=0}^3 \int_0^{\frac{1}{4}} X_0^2\left(\frac{k}{4} + s\right) \sin\left(2\pi\left(\frac{k}{4} + s\right)\right) ds \\
&= - \sum_{k=0}^3 \int_0^{\frac{1}{4}} X_0^2\left(\frac{k}{4} - s\right) \sin\left(2\pi\left(\frac{k}{4} - s\right)\right) ds \\
&= \sum_{k=0}^3 \int_{\frac{1}{4}}^0 X_0^2\left(\frac{k}{4} + s\right) \sin\left(2\pi\left(\frac{k}{4} + s\right)\right) ds \\
&= - \int_0^1 X_0^2(s) \sin(2\pi s) ds,
\end{aligned}$$

which yields

$$\int_0^1 X_0^2(s) \sin(2\pi s) ds = 0.$$

Next, similar calculations show that

$$\int_0^{\frac{1}{2}} X_0^2(s) \cos(2\pi s) ds = 0 \text{ and } \int_{\frac{1}{2}}^1 X_0^2(s) \cos(2\pi s) ds = 0$$

so that, indeed,

$$\int_0^1 X_0^2(s) \cos(2\pi s) ds = 0.$$

Next we see that

$$\begin{aligned}
\int_0^1 X_0^2(s) \cos(4\pi s) ds &= \sum_{k=0}^7 \int_0^{\frac{1}{8}} X_0^2\left(\frac{k}{8} + s\right) \cos\left(4\pi\left(\frac{k}{8} + s\right)\right) ds \\
&= \sum_{k=0}^7 (-1)^{2k+1} \int_0^{\frac{1}{8}} X_0^2\left(\frac{k}{8} - s\right) \cos\left(4\pi\left(\frac{k}{8} - s\right)\right) ds \\
&= \sum_{k=0}^7 \int_{\frac{1}{8}}^0 X_0^2\left(\frac{k}{8} + s\right) \cos\left(4\pi\left(\frac{k}{8} + s\right)\right) ds = - \int_0^1 X_0^2(s) \cos(4\pi s) ds.
\end{aligned}$$

As for the last integral, notice that

$$X_0^2(s) \sin(4\pi s) > 0 \text{ on } [0, 1) \setminus \{0, \frac{1}{4}, \frac{1}{2}, \frac{3}{4}\}$$

and, hence, that

$$\int_0^1 X_0^2(s) \sin(4\pi s) ds > 0,$$

as announced. As the linear heat equation and any reparametrization maintains the symmetries (8.1) and (8.2), it can be inferred that the same integral (spectral) properties are enjoyed by the approximants $X^n(t)$ and for all times $t > 0$, regardless of the value of $n \in \mathbb{N}$. We now estimate the components. Recall that

$$Y(t) = e^{-\frac{t-kh}{L^2(X_k^n)} \partial_{ss}} R(X_k^n), \quad t \in [kh, (k+1)h).$$

It follows that

$$\begin{aligned}
\|Y^j(t)\|_\infty &\leq \|Y^j(t)\|_{1,2} \leq e^{-\frac{4\pi^2(t-h)}{L^2(X_k^n)}} \|R(X_k^n)\|_{1,2} \leq e^{-\frac{4\pi^2(t-h)}{L^2(X_k^n)}} \|R(X_k^n)\|_{1,\infty} \\
&\leq 2e^{-\frac{4\pi^2(t-h)}{L^2(X_k^n)}} L(X_k^n), \quad t \in [kh, (k+1)h), \quad j = 1, 2.
\end{aligned}$$

Here we used the facts that

$$\|R(X_k^n)_s\|_\infty = L(X_k^n) \text{ and that } \|R(X_k^n)\|_\infty \leq \frac{L(X_k^n)}{2},$$

where the latter follows from the symmetries of the evolving curves about the x - and y -axis as well as the fact that the diameter of a closed curve is at most half its length. Now the decay enjoyed by $Y^1(t)$ is precisely that suggested by the inequality since the

$$\langle Y^1, \cos(2\pi \cdot) \rangle \neq 0,$$

while that of Y^2 has a factor of $16\pi^2$ instead of $4\pi^2$ since

$$\langle Y^2, \varphi(2\pi \cdot) \rangle = 0, \varphi = \cos, \sin.$$

This shows that the aspect ratio of the evolving curve tends to zero as the curve shrinks to a point while maintaining its symmetries. The rescaled limit does therefore have to be the doubly covered segment of length 1 that enjoys x - and y -axis symmetry as desired. \square

Remark 8.2. *It was already conjectured in [1] that the limiting (normalized) curvature of a symmetric figure eight curve be that of a doubly covered segment. In this case the (normalized) curvature does not converge to its asymptotic limit in the L^1 -topology. By [1] all (closed) curves for which it does must converge to a (smooth) homotetic solution. We now know that a doubly covered segment instantaneously shrinks to a point and can therefore also be thought as a very fast self-similar shrinker.*

Remark 8.3. *In [12], Grayson studied the evolution of planar figure eight shapes (in his definition, curves with exactly a double point and vanishing signed area) and showed that the isoperimetric ratio $\frac{L^2}{A}$ tends to infinity as the extinction time is approached if and only if the two loops enclose regions of equal area.*

Remark 8.4. *For an initial curve to converge to a doubly covered segment, it is enough to require lesser symmetry for the initial datum Y_0 as, for instance, central symmetry*

$$Y_0\left(\frac{1}{2} + s\right) = -Y_0\left(\frac{1}{2} - s\right), \quad s \in [0, 1),$$

or y -axis symmetry

$$Y_0\left(\frac{1}{2} + s\right) = \begin{bmatrix} -1 & 0 \\ 0 & 1 \end{bmatrix} Y_0\left(\frac{1}{2} - s\right),$$

which ensure that the total signed area vanishes all along the evolution as all the approximants and hence the limit preserve these symmetries. In this case, however, the location and direction of the limiting segment is not immediately available. See Figure 5 for such situations. The additional symmetries enjoyed by X_0 make sure that the limiting segment is on the x -axis in the chosen coordinates.

Remark 8.5. *The discussion of the long time behavior of the infinity loop and the construction of the solution show that the curve shortening flow exhibits a long time behavior that could be described as qualitatively of heat type. By this we mean that a generic initial datum that has a persistent non-zero projection onto the first non-constant modes will shrink to a circular point as the first mode will dominate the decay. Clearly the effect of diffusion is amplified and sped up by the length dependent diffusivity which also causes finite extinction time. For a curve to shrink to a non-circular point, it will need to have qualitative properties (symmetries) which prevent the first non-constant modes to dominate the evolution. The infinity loop considered above is such an example. We will show in the section dedicated to numerical experiments that small perturbations of these symmetries lead back to convergence to a round point.*

9. SYMMETRIES AND LONG TIME BEHAVIOR

9.1. Symmetries. Any parametrization X of an immersed curve will have velocity X_r and acceleration X_{rr} . These depend on the way the curve is traversed and do not immediately provide intrinsic geometric information about the immersed curve. The velocity can, however, be split into the product of speed and direction

$$X_r = |X_r| \frac{X_r}{|X_r|},$$

leading to a decomposition of the acceleration

$$X_{rr} = \frac{d}{dr} |X_r| \frac{X_r}{|X_r|} + |X_r| \left(\frac{X_r}{|X_r|} \right)_r = |X_r|_r \frac{X_r}{|X_r|} + |X_r|^2 k(X)$$

into a tangential (parametrization dependent) and a normal component. The curvature $k(X)$ is the acceleration experienced by traversing the curve at a constant unit speed. As such, it is an intrinsic property of an immersed curve and not a manifestation of the specific way the curve is run through. It is, however, not an intrinsic property of the trace set $X(I) \subset \mathbb{R}^d$, which by itself cannot be considered an immersed curve. Parametrized curves are not simple subsets of \mathbb{R}^d . They are topological spaces with respect to the topology induced by their parametrization equivalence class. It follows that distinct curves X and Y with the same trace set, i.e. for which $X(I) = Y(I)$, need not be the same topological space and, hence, manifold. While embedded curves also carry the topology induced by their parametrization classes, this topology does coincide with the “natural” topology of their trace set, which is the one induced by the ambient space \mathbb{R}^d . Immersed curves, by contrast, have topologies that do not coincide with the induced topologies of their trace sets. To see this, take an infinity like shape: any open neighborhood of the crossing point in the topology induced by \mathbb{R}^2 , will contain two crossing curve segments. That is not the case for any of the two possible curve topologies corresponding to the two distinct ways in which the trace set can be run across as depicted in Figure 3. These topologies are what distinguishes their CSF evolutions. See Figure 4. If the CSF is interpreted in a sense that only uses the initial trace set as a topological subspace of the ambient space, then uniqueness may be lost for any concept of weak solution.

This shows that symmetries enjoyed by the trace set of an initial curve in the ambient space do not suffice to determine the evolution of the curve by the CSF. One indeed needs to consider the symmetries of its normalized parametrization since curves with the same trace set can enjoy different symmetries as immersed manifolds. Again we are confronted with the fact that embedding symmetries coincide with ambient space symmetries, while immersion symmetries cannot be inferred from ambient symmetries. In Figure 3, the curve X_l on the left satisfies

$$X_l\left(\frac{1}{2} + s\right) = \underbrace{\begin{bmatrix} -1 & 0 \\ 0 & -1 \end{bmatrix}}_{R_1} X_l\left(\frac{1}{2} - s\right), \quad s \in [0, 1),$$

while the one on the right

$$X_r\left(\frac{1}{2} + s\right) = \underbrace{\begin{bmatrix} -1 & 0 \\ 0 & 1 \end{bmatrix}}_{R_c} X_r\left(\frac{1}{2} - s\right), \quad s \in [0, 1).$$

The common trace set $C = X_l(I) = X_r(I)$, however, satisfies

$$R_1(C) = C, \quad R_c(C) = C, \quad \text{and} \quad -R_1(C) = C.$$

We also observe that $\kappa_{tot}(X_l) \neq \kappa_{tot}(X_r)$.

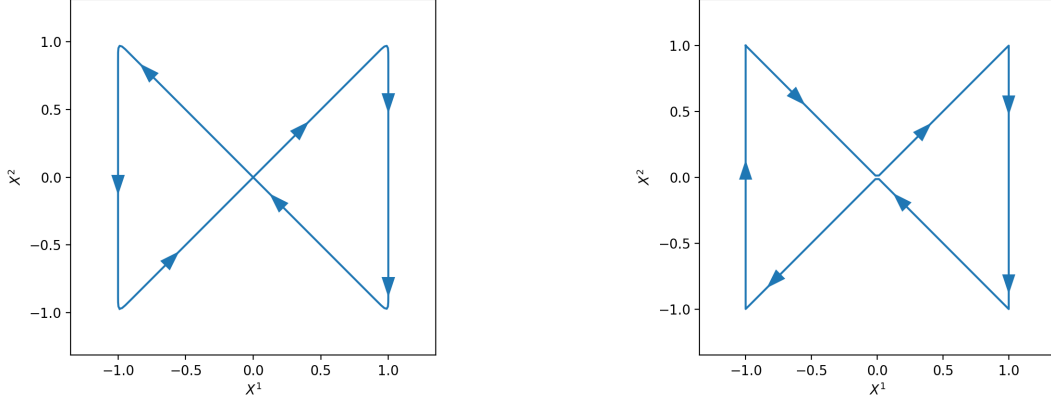


FIGURE 3. Two distinct immersed curves sharing the same trace set. They do carry different topologies that are both distinct from the topology induced by the ambient plane.

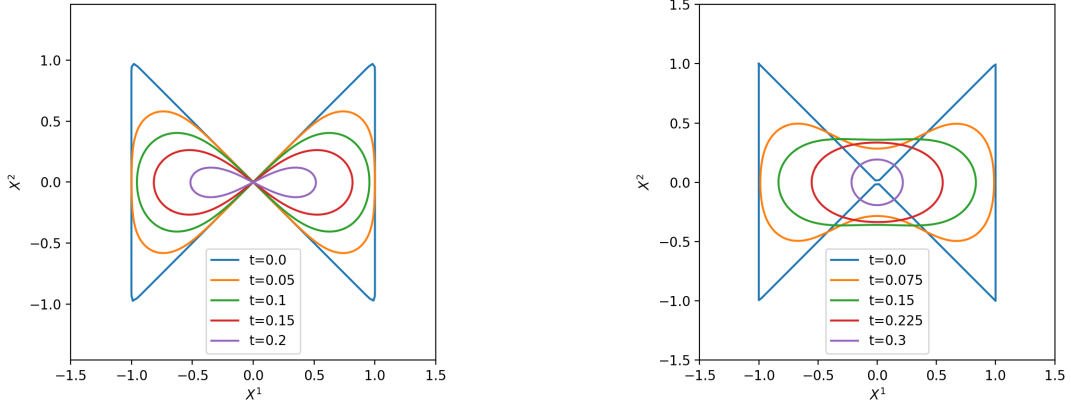


FIGURE 4. Snapshots of the evolution of two topologically distinct curves sharing the same trace set.

9.2. Long Time Behavior. It was shown by Altschuler [2] that space curves, i.e. curves in \mathbb{R}^3 , that develop a singularity, are asymptotic to planar Abresch-Langer homotetic solutions if the singularity is of type I (and thus not a cusp). Type II singular behavior is also studied and shown to lead to Gream Reapers by blow up around points where the curvature explodes as the singular time is approached. This shows that space curves of the CSF flow constructed in this paper shrink to a point in a self-similar fashion (asymptotic to an Abresch-Langer curve, which include multiply covered circles) or to a $2m$ -covered segment for $m \geq 1$. The latter can be considered as a degenerate Abresch-Langer curve with “rotation index” m and such that the curvature closes up in m periods, and, hence, in some sense, a degenerate m -covered circle.

10. A NUMERICAL SCHEME

The inspiration for the numerical method to be described shortly is to be found in the construction of the solution presented earlier and in the smoothing properties of the curve shortening flow. We think of a discrete curve as a n -tuple of points $\mathbb{X} = (X_0, X_1, \dots, X_{n-1})$. As we only consider closed curves,

we can visualize \mathbb{X} as the polygon $P(\mathbb{X})$ obtained by connecting X_i to $X_{(i+1) \bmod n}$ for $i = 0, \dots, n-1$. The length of the curve \mathbb{X} is taken to be the length of the polygon $P(\mathbb{X})$ so that

$$L(\mathbb{X}) = L(P(\mathbb{X})) = \sum_{i=0}^{n-1} |X_{(i+1) \bmod n} - X_i|.$$

Given a discrete closed curve \mathbb{X} , its natural arclength parametrization is given by

$$X_k = X(l_k), k = 0, \dots, n-1,$$

where arclength is itself given by

$$l_k = \sum_{i=0}^{k-1} |X_{(i+1) \bmod n} - X_i|, k = 1, \dots, n,$$

with the understanding that $l_0 = 0$. It can naturally be extended to a continuous parametrization of $P(\mathbb{X})$ by setting

$$X(t) = \frac{t - l_k}{l_{k+1} - l_k} X_k + \frac{l_{k+1} - t}{l_{k+1} - l_k} X_{(k+1) \bmod n},$$

for $t \in (l_k, l_{k+1})$ and $k = 0, \dots, n-1$. In order to simplify the computation of curvature, needed for the evolution, we replace the non-uniform discrete parametrization of $P(\mathbb{X})$ by a uniform one comprised of $N \geq n$ points $\mathbb{Y} = (Y_0, \dots, Y_{N-1})$ along $P(\mathbb{X})$ such that

$$d_{P(\mathbb{X})}(Y_k, Y_{k+1}) = \frac{L(\mathbb{X})}{N}, k = 0, \dots, N-1,$$

where $d_{P(\mathbb{X})}$ is the distance measured along $P(\mathbb{X})$.

Remark 10.1. *If \mathbb{X} is a discretization of a smooth curve of some order (of accuracy) $p > 1$, then so is \mathbb{Y} . Thus the reparametrization step does not affect accuracy.*

Proof. If $\mathbb{X}^h = \{x_i^h \mid i = 0, \dots, n(h)-1\}$ is an approximating set sequence for a curve $\Gamma \subset \mathbb{R}^d$ such that

$$d(x_i^h, \Gamma) \leq Ch^p, i = 0, \dots, n(h)-1, h > 0,$$

then, for any point x along the polygon $P(\mathbb{X}^h)$ it holds that $x = (1 - \tau)x_i^h + \tau x_{(i+1) \bmod n(h)}^h$ for some $i \in \{0, \dots, n(h)-1\}$ and $\tau \in (0, 1)$. Thus we have that

$$d(x, \Gamma) \leq (1 - \tau)d(x_i^h, \Gamma) + \tau d(x_{(i+1) \bmod n(h)}^h, \Gamma) \leq Ch^p,$$

as claimed. □

We denote the constructed polygon $\mathbb{Y} \in \mathbb{R}^N$ by $R_N(\mathbb{X})$ as it corresponds to the reparametrization operator R used earlier in the continuous setting. It is then natural to define the curvature $k(\mathbb{X})$ of \mathbb{X} by

$$k(\mathbb{X}) = \frac{1}{L^2(\mathbb{X})} \mathcal{F}_N^{-1} D_N^2 \mathcal{F}_N R_N(\mathbb{X}),$$

where \mathcal{F}_N denotes the discrete Fourier transform and D_N denotes the diagonal matrix with diagonal entries given by $-2\pi i k$ for $k = -\frac{N}{2}, \dots, \frac{N}{2} - 1$. In this case D_N^2 is the symbol of the spectral discrete Laplacian. With these notations the numerical scheme reads

$$\begin{cases} \mathbb{X}^{n+1} = \mathcal{F}_N^{-1} e^{-\frac{h}{L^2(\mathbb{X}^n)} D_N^2} \mathcal{F}_N R_N(\mathbb{X}^n), & n \geq 0, \\ \mathbb{X}^0, & \text{given,} \end{cases} \quad (10.1)$$

with a discrete time step $h > 0$.

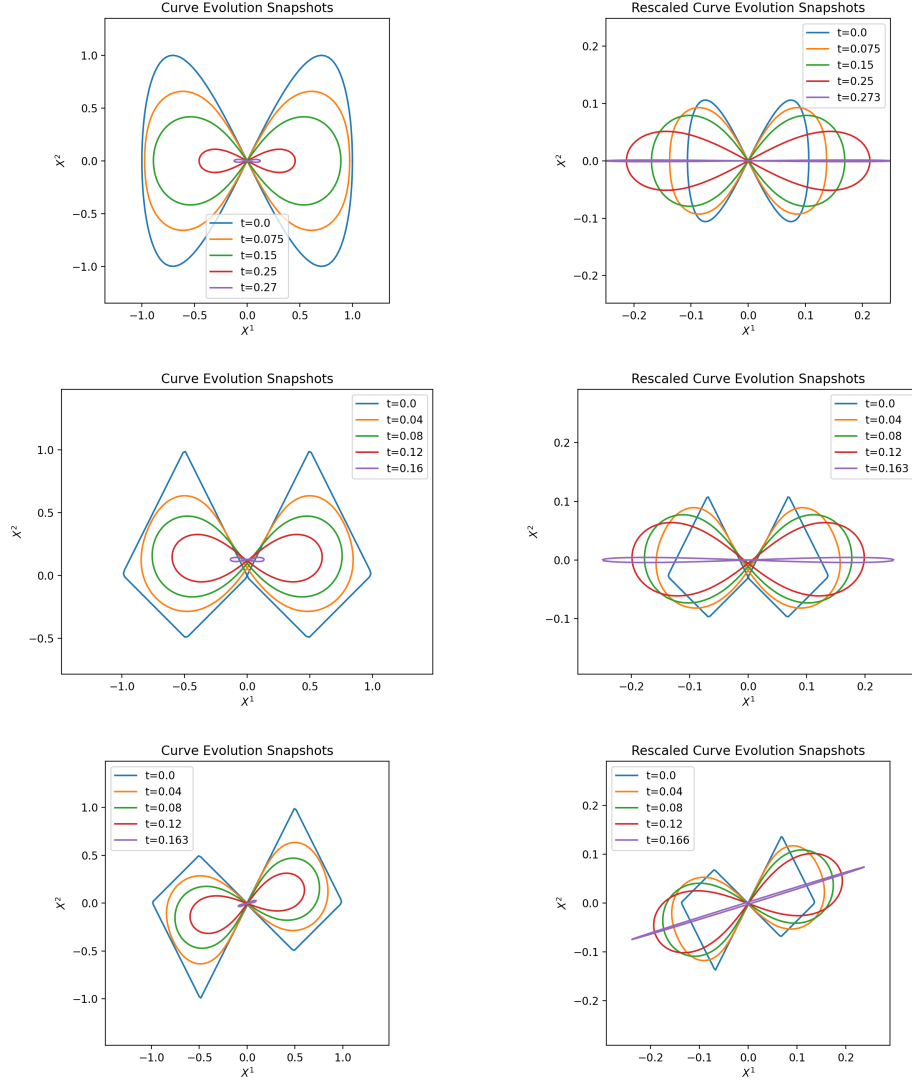


FIGURE 5. On the left, the evolution of different initial infinity-like curve (in blue) is shown, while, on the right, the same curves are rescaled to have unit length to clearly show the asymptotic shape in the singularity. In the second example the rescaled curves are recentered around their center of mass since, in this case, the curve evolution moves the center of the shape due to a lack of symmetry with respect to the x -axis.

11. NUMERICAL EXPERIMENTS

11.1. Infinity Like Shapes. We consider three infinity-like shapes: one with both x -axis and y -axis symmetries, one with only y -axis symmetry and one with central symmetry. These evolutions, depicted in Figure 5, exhibit the expected asymptotic behavior, i.e. convergence to a point not asymptotically circular, but rather in the shape of a doubly covered segment. Shown are snapshots of the actual curve evolution and a version rescaled to have length one and recentered in the center of mass of the curve. If we modify the infinity shape by adding a small bump to the loop on the right. This break of symmetry is enough to change the long time behavior of the solution as shown in Figure 6. The curve now shrinks to a round point.

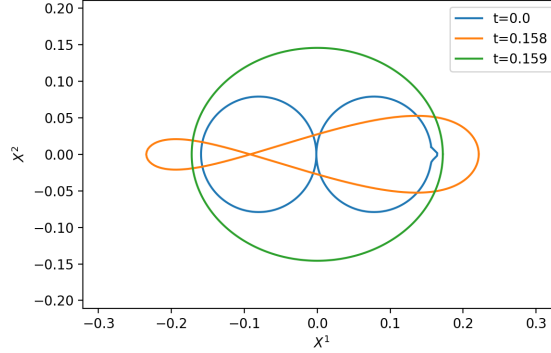


FIGURE 6. Evolution of a slightly perturbed infinity shape. Curves are rescaled to have unit length.

11.2. A Convoluting Curve. In Figure 7 we show the evolution of curve with many self-intersections originating in the immersed curve determined by the parametrization given by

$$X_0(s) = (3 \cos(3s), \sin(8s)), \quad s \in I.$$

This curve evolves by reducing the number of extremity points as expected and, in doing so, it also reduces the number of intersections. This does not always happen via the formation of singularities. Singularities are only observed at time $t \simeq 0.282$, when four loops are shedded simultaneously, and at time $t \simeq 0.54$, when two additional loops disappear. At the extinction time, the curve is asymptotic to a doubly covered segment after having simplified to an infinity loop. In Figure 8 we also plot the corresponding evolution of length and total absolute curvature. The singular times are clearly visible in both graphs. The behavior of the numerical total absolute curvature shortly before the singularity times is a rough approximation since the loops disappear in the singularities and a fixed number of discrete parameter points are used in the computation that do not suffice to resolve the total curvature of a small loop.

11.3. Linear Diffusion. Here we highlight the fact that loop-shedding is not a consequence of the nonlinear nature of the CSF as it is observed also when a curve is evolved by pure diffusion. This is depicted in Figure 9, where an initial curve consisting of two adjacent circles touching in the origin and immersed like an infinity shape with crossing is evolved by the heat equation with diffusivity determined by its initial length

$$X_t = \frac{1}{L(X_0)^2} X_{ss}, \quad X(0) = X_0. \quad (11.1)$$

The left circle is taken with radius $\frac{1}{4}$ and right circle has radius $\frac{3}{4}$. This underscores the insight that singularity formation at the level of the curve does not stem from a singularity in any component of its parametrization but rather is due to certain zero coalescence events as explained earlier in the paper.

REFERENCES

- [1] U. Abresch and J. Langer. The normalized curve shortening flow and homothetic solutions. *J. Differential Geom.*, 23(2):175–196, 1986.
- [2] Steven J. Altschuler. Singularities of the curve shrinking flow for space curves. *J. Differential Geom.*, 34(2):491–514, 1991.

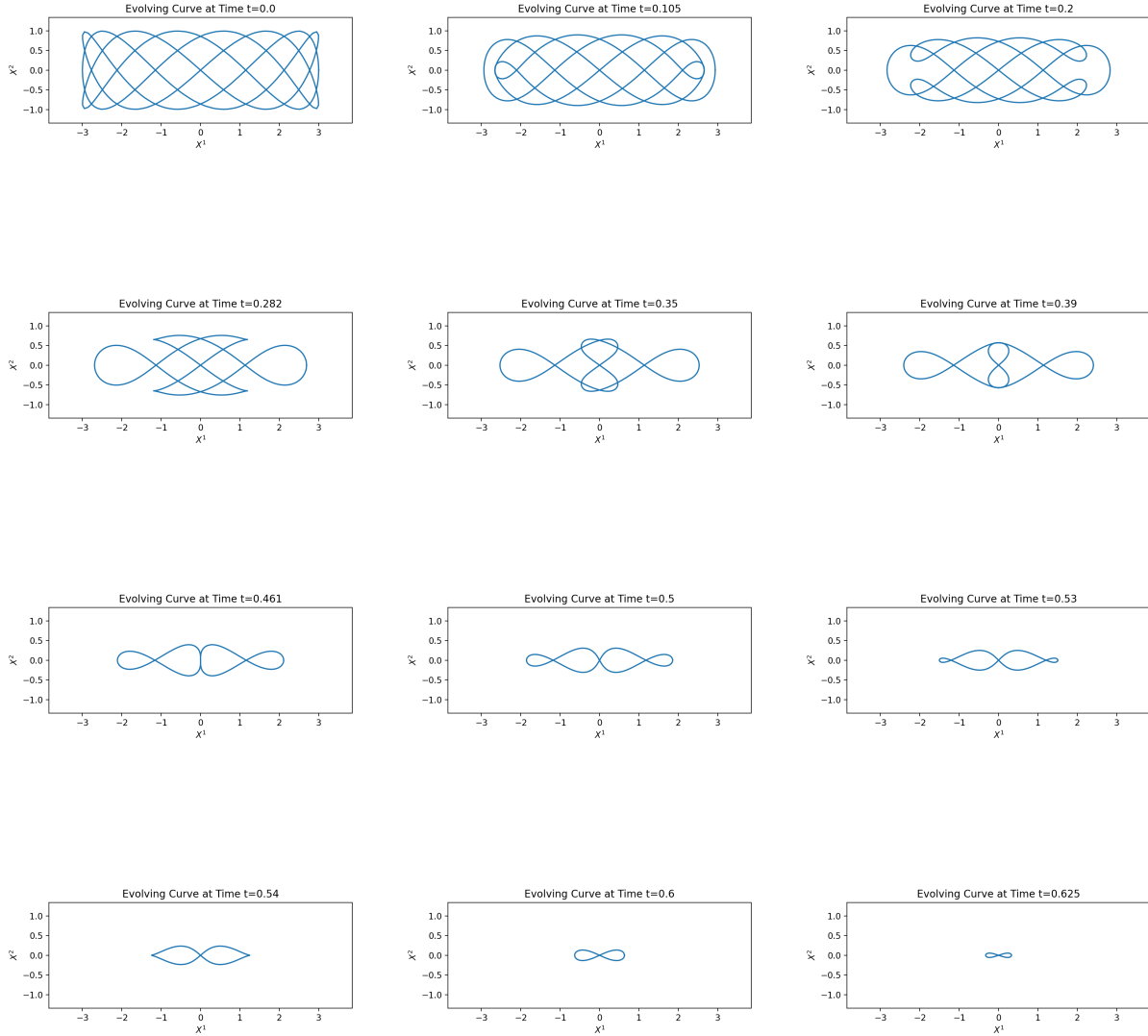


FIGURE 7. Evolution of a convoluted curve with initial parametrization given by $X_0(r) = (3 \cos(6\pi r), \sin(16\pi r))$, $r \in [0, 1)$. There are two singularity times during this evolution, the first sheds four loops simultaneously ($t \simeq 0.282$) and the second two ($t \simeq 0.54$).

- [3] Steven J. Altschuler and Matthew A. Grayson. Shortening space curves and flow through singularities. *J. Differential Geom.*, 35(2):283–298, 1992.
- [4] Sigurd Angenent. Parabolic equations for curves on surfaces. i. curves with p -integrable curvature. *Ann. of Math. (2)*, 132(3):451–483, 1990.
- [5] Sigurd Angenent. On the formation of singularities in the curve shortening flow. *J. Differential Geom.*, 33(3):601–633, 1991.
- [6] Sigurd Angenent. Parabolic equations for curves on surfaces. II. Intersections, blow-up and generalized solutions. *Ann. of Math. (2)*, 133(1):171–215, 1991.
- [7] Kenneth A. Brakke. *The motion of a surface by its mean curvature*, volume 20 of *Mathematical Notes*. Princeton University Press, Princeton, N.J., 1978.

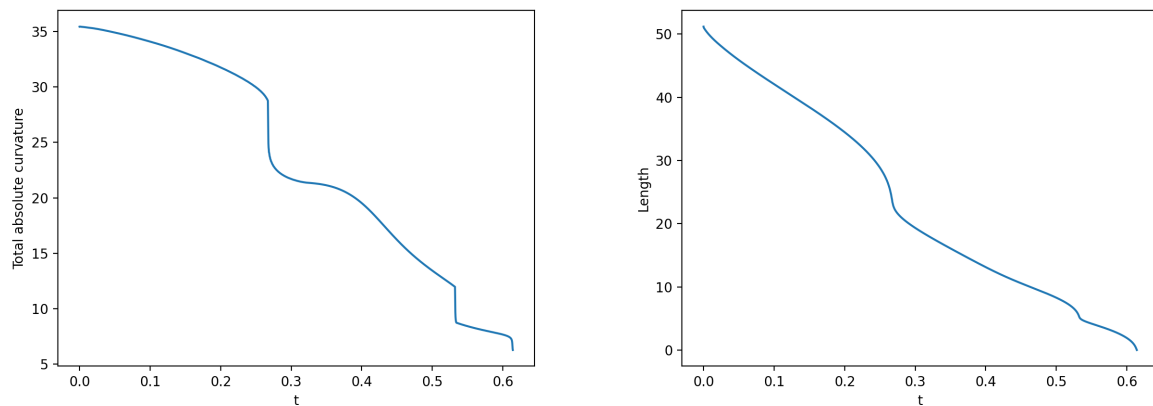


FIGURE 8. Length and total absolute curvature along the orbit of the convoluted curve of Figure 7

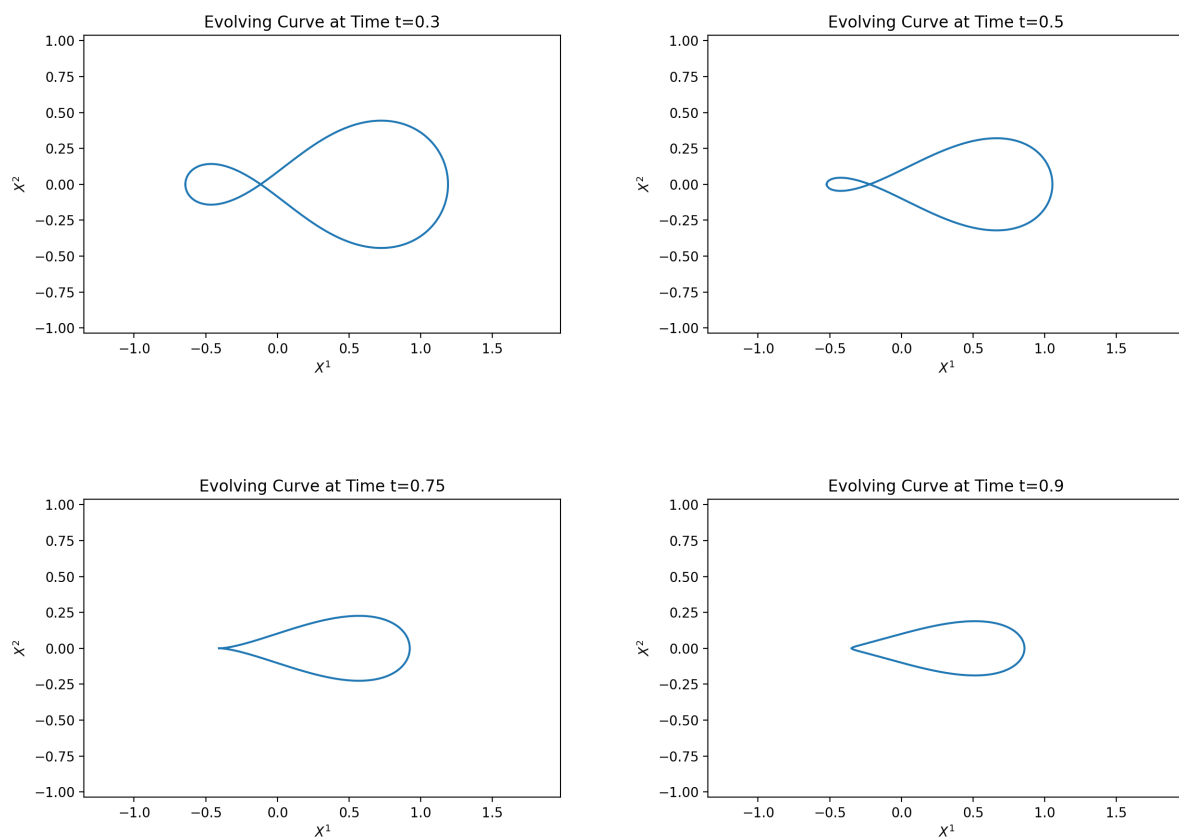


FIGURE 9. Evolution of an infinity like shape consisting of two circles with different radii touching in the origin by the simple heat flow (11.1).

- [8] M. Gage and R. S. Hamilton. The heat equation shrinking convex plane curves. *J. Differential Geom.*, 23(1):69–96, 1986.
- [9] M. E. Gage. Curve shortening makes convex curves circular. *Invent. Math.*, 76(2):357–364, 1984.
- [10] Michael E. Gage. An isoperimetric inequality with applications to curve shortening. *Duke Math. J.*, 50(4):1225–1229, 1983.
- [11] Matthew A. Grayson. The heat equation shrinks embedded plane curves to round points. *J. Differential Geom.*, 26(2):285–314, 1987.
- [12] Matthew A. Grayson. The shape of a figure-eight under the curve shortening flow. *Invent. Math.*, 96(1):177–180, 1989.
- [13] Hoeskuldur P. Halldorsson. Self-similar solutions to the curve shortening flow. *Trans. Amer. Math. Soc.*, 364(10):5285–5309, 2012.
- [14] Gerhard Huisken. Asymptotic behavior for singularities of the mean curvature flow. *J. Differential Geom.*, 31(1):285–299, 1990.
- [15] C. Mantegazza. *Lecture Notes on Mean Curvature Flow*. Progress in Mathematics. Springer Basel, 2011.
- [16] J. W. Milnor. On the total curvature of knots. *Ann. of Math. (2)*, 52:248–257, 1950.
- [17] John M. Sullivan. *Curves of Finite Total Curvature*, pages 137–161. Birkhäuser Basel, Basel, 2008.

UNIVERSITY OF CALIFORNIA, IRVINE, DEPARTMENT OF MATHEMATICS, 340 ROWLAND HALL, IRVINE, CA 92697-3875, USA

Email address: gpatrick@math.uci.edu